Big data reveals deep associations in physical examination indicators and can help predict overall underlying health status

Haixin Wang[1#], Ping Shuai[2#], Yanhui Deng[1#], Jiyun Yang[1], Shanshan Zhang[1], Yi Yin[1], Lin Wang[2], Dongyu Li[2], Tao Yong[3], Yuping Liu[2*] and Lulin Huang[1*]

[1]The Key Laboratory for Human Disease Gene Study of Sichuan Province, Department of Clinical Laboratory, Sichuan Provincial People's Hospital, School of Medicine, University of Electronic Science and Technology of China, Chengdu, China;
[2]Health Management Center & Physical Examination Center of Sichuan Provincial People's Hospital, School of Medicine, University of Electronic Science and Technology of China, Chengdu, China;
[3]Medical Information Center of Sichuan Provincial People's Hospital, School of Medicine, University of Electronic Science and Technology of China, Chengdu, China.

# These authors contributed equally.

*Correspondence should be addressed to: Lulin Huang, Ph.D. Email: huangluling@yeah.net or Yuping Liu, Email: liuyuping555@126.com

32 The First Ring Road West 2, Chengdu, Sichuan 610072, China,

Phone: 86-28-87393375,

Fax: 86-28-87393596.

Abstract

Because of lacking of the systematic investigation of correlations between the physical examination indicators (PEIs), currently most of them are independently used for disease warning. This results in very limited diagnostic values of general physical examination. Here, we first systematically analyzed the correlations between 221 PEIs in healthy and in 34 unhealthy states in 803,614 peoples in China. We revealed rich relevant between PEIs in healthy physical status (7,662 significant correlations, 31.5% of all). However, in disease conditions, the PEI correlations changed. We further focused on the difference of these PEIs between healthy and 35 unhealthy physical status, 1,239 significant PEI difference were discovered suggesting as candidate disease markers. Finally, we established machine learning algorithms to predict the health status by using 15%-16% PEIs by feature extraction, which reached 66%-99% precision predictions depending on the physical state. This new encyclopedia of PEI correlation provides rich information to chronic disease diagnosis. Our developed machine learning algorithms will have fundamental impact in practice of general physical examination.

The comprehensive primary healthcare system has had a broader impact on human health compared to clinical medical treatment[1-4]. Health examinations help those who are healthy to improve their understanding of their own physical functions and maintain their health status, and inform those as to the health benefits conferred by changing unhealthy habits and avoiding risk factors that can lead to disease[5]. Physical examinations can help minimize the distress of diseases[6]. With the population size grows and ages, people's healthcare needs are constantly increasing, and health-care provisions are becoming more sophisticated and in parallel, more costly[7].

Health examinations are common elements of healthcare in developed countries[8]. These checks consist of general blood examination, urine examination, blood glucose examination, blood lipid examination, renal function examination and so on. However, currently, the physical examination report is assessed mainly based on one or two independent physical examination indicators (PEIs), which can only provide very limited information for physical examiners about their healthy condition or disease diagnosis[9-11]. The correlations between PEI in different physical states (i.e. healthy, hypertension, diabetes) have not been systematically investigated, even though they are expected to provide valuable information for public health care, for example by defining a small set of easily measurable PEIs that can be used in the accurate diagnosis of a disease before the disease phenogenesis.

The recent explosion of available health data promises to transform healthcare by improving care quality and as such, improving population health while constraining escalating costs[12]. Health examination centers generate systematic big data that has the capacity to reveal otherwise undetected underlying health issues[13-14]. In clinical, there is growing investment in developing big data applications for medical care, such as those based on artificial intelligence (AI) to diagnosis diseases based on clinical images[15-17]. Although AI can save cost and improve efficiency, especially for early diagnosis and prevention of chronic diseases[18], because of insufficient systematic analysis of PEIs in physical status, currently no prediction models were generated for physical status predictions based on PEIs.

As China’s 2009 health-care reform has made impressive progress in expansion of insurance coverage, now general physical examination industry accumulates big data[19]. By using a large dataset of general health examination of Chinese population, the present study had three main aims: to

determine the correlations among PEIs in healthy and unhealthy (namely, those with underlying chronic disease) patients; to elucidate the relationship between chronic disorders and normal individuals for these PEIs to discovery candidate disease markers; to develop machine learning models that can predict individual health status using a refined set of PEIs. To address these points, we included physical examination data from 80,3614 individuals who visited one health examination center between 2013 and 2018 in China. We included data from 221 PEIs associated with 35 physical conditions, with the majority unhealthy physical states being due to chronic disease.

Results

Study population

The study population was mainly from the Chengdu Plain, Sichuan, P.R. China (102.54°E ~104.53°E and 30.05°N ~31.26°N). We included 803,614 individuals who attended the Health Management Center & Physical Examination Center of Sichuan Provincial People's Hospital in China between 2013 and 2018. The participants represented 35 healthy states based on either a healthy status or the presence of an underlying disease condition (unhealthy status). Specifically, the study population included 711,928 healthy participants, 46,981 patients with hypertension, 11,745 patients with diabetes and 32,960 with other unhealthy status (mainly are chronic disease) (Table 1). We included 221 PEIs in our analyses, which comprised patient demographic information (age and sex) and life-style indicators (alcohol consumption, tobacco use, etc.) (Extended data Table 1).

PEI correlations in participants with a healthy physical status

We first aimed to explore the PEI correlations in healthy status to give a landscape. Among 221 PEIs, we found 7,662 significant correlations (P<0.05/ 24,322 PEI pairs=2×10^{-6}) in all 24,322 PEI pairs correlations (31.5%) (Table 1, Supplementary Table 1) in those with a healthy physical status (N=711,928, mean age 41.4, female=45.7%). This finding suggests a wide range of correlations between PEIs (Fig.1). The top 50 correlated PEIs included sex, age, red blood cell count, prealbumin (PAB), history of alcohol intake (alcohol consumption, drinking), alkaline phosphatase level (ALP), tobacco use (smoking) and so on (Fig. 1a). Among the 221 PEIs, the number of significantly correlated PEIs also suggested rich correlations between PEIs (Fig. 1b). Of these identified correlations among PEIs in healthy status, some of them are consistent with the reported literatures, but most of them are newly discovered in this study.

General inspection PEIs showed rich relevance to each other or to other PEIs. For example, sex showed the richest PEI correlations (151 PEI pairs, males vs. females), including hemoglobin (Hb), creatinine, uric acid (UA), drinking, smoking, body mass index (BMI) and etc., which reflect the differences in body shape, physique and living habits between males and females (Fig. 1, Fig. 2, Supplementary Table 1). Age also showed strong PEI correlations (125 PEI pairs), such as estimated glomerular filtration rate (eGFB), systolic pressure (SBP), diastolic pressure (DBP), albumin (Alb), and low-density lipoprotein (LDL-C). These findings suggest that with increasing age, body functions systematically change (Fig. 1, Fig. 2, Supplementary Table 1). We also found 124 PEI correlations with BMI which reflects the strong influence of body shape on PEIs, including UA, high-density lipoprotein (HDL-C), SBP, and DBP (Fig. 1, Fig. 2, Supplementary Table 1). Blood pressure (BP), which has many physiological meanings, we identified a set of PEIs that correlated with blood pressure (BP), including 125 PEIs for DBP and 124 PEIs for SBP (Fig. 1, Fig. 2, Supplementary Table 1). Intraocular pressure (IOP) is an important factor for the diagnosis of glaucoma[8-9]. We found 79 PEIs that were weakly correlated with IOP of the left eye (IOP-L), including IOP of the right eye (IOP-R) SBP, DBP, Alb, BMI, TG, ApoB, drinking, and TC. Similar to IOP-L, 73 PEIs were weakly correlated with IOP-R (Fig. 1, Fig. 2, Supplementary Table 1).

As expected, blood lipid PEIs display many correlations. For example, 119 PEIs correlated with triglyceride (TG) (Fig. 1, Fig. 3, Supplementary Table 1). We found 122 PEIs that correlated with HDL-C, with many negative correlations, including TG, UA, and BMI (Fig. 1, Fig. 2, Supplementary Table 2). The correlation patterns between LDL and HDL showed a specific opposite trend (Fig. 1, Fig. 2, Supplementary Table 1). Out of expected, living habits have a profound impact on our body. Consistently we detected 130 PEIs that correlated with drinking, such as sex, smoking, Hb and UA (Fig. 1, Fig. 2, Supplementary Table 1). Similarly, 128 PEIs were correlated with smoking, including drinking, sex and age (Fig. 1, Fig. 2, Supplementary Table 1). We also detected 58 PEIs that weakly correlated with exercise habits (e-habits), including age, eGFB, and SBP (Fig. 1, Fig. 2, Supplementary Table 1). Tumor marker expression can indicate the occurrence and development of tumors. We detected weak correlations between several tumor markers and PEIs. For example, 88 PEIs were correlated with cytokeratin-19-fragment CYFRA21-1 (CYFRA 21-1); 83 PEIs were correlated with tumor-supplied group factors (TSGF); 64 PEIs were correlated with neuron-specific enolase (NSE);

and 64 PEIs were correlated with complexed prostate special antigen (C-PSA) (Fig. 1, Fig. 2, Supplementary Table 1).

PEI correlations in individuals with an unhealthy physical status

Next, we examined the PEI correlations in 34 unhealthy physical states. In this analysis, we also identified rich correlations in these unhealthy physical states (Table 1). Compared with the healthy physical state, we found fewer significant correlations in PEIs in those with an unhealthy physical status, which might be caused by sample size effect (Table 1, Supplementary Table 2-S35). Each unhealthy physical state has its only correlation spectrum and most of them are newly discovered in this study. For example, in the hypertension population, we found 4,413 significant correlations in the 221 PEIs of 24,322 PEI pairs (18.3%) (Supplementary Table 2). The PEI with increased correlations included monocytes (MON) (70 in hypertension vs six in healthy physical state, the same below), quantitative detection of hepatitis B virus DNA (HBV-DNA) (76 vs 33), quantitative detection of hepatitis C virus RNA (HCV-RNA) (49 vs 8), etc. (Supplementary Table 2). Those with both hypertension and coronary heart disease (hypertension+coronary) had an increased correlation of RH blood group compared with the healthy cohort (41 vs 9 in normal). Conversely, the numbers of correlations in homocysteine (Hcy) were greatly reduced in unhealthy versus healthy patients (2 vs 120). In diabetes, 10 PEI pairs increased while the remaining 195 PEI pairs decreased; the increased PEIs including MON (41 vs 6), HCV-RNA (42 vs 8), anti-Sc70 (59 vs 31) and HCV-cAg (35 vs 10) (Supplementary Table 17). These results suggest that under the unhealthy status, the PEIs have changed systematically. Each disease has its own specific PEI spectrum.

We next explored the correlation networks among the PEIs using a qgraph[8,10], which would show the LinkMode among PEIs. In the healthy status, we found that the PEIs showed rich interactions with both positive and negative directions (Fig. 3). In the unhealthy physical states, each of them showed its unique interaction networks with PEIs (Extended Data Figure 2 showed the network of hypertension and diabetes). These results show that there is a dependency relationship between multiple indicators in each physical state, which can be used with combination in the assessment of physical health.

Candidate PEI markers for unhealthy physical status

To verify and discovery new candidate biomarkers or the impact of living habits for disease early diagnosis, we next calculated the difference of each of the 221 PEIs between healthy and unhealthy physical states. In total, we found 1,239 significantly different PEI pairs between healthy and 34 unhealthy physical status ($P<0.05/34=0.0014$, adjust for 34 unhealthy physical status) (Table 1, Fig. 4, Supplementary Table 36). For example, 112 PEIs were significantly different between patients with hypertension and healthy people, 100 PEIs were different between hypertension+diabetes and healthy people, and 91 PEIs were different between diabetes and the healthy people. Some of them are consistent with previous findings and the rest of them are newly discovered.

For many of the 221 PEI, we detected difference between healthy and unhealthy physical status, especially in PEIs involved in physique, lifestyles, blood lipids (Fig. 4, Supplementary Table 36). For example - BMI, we found differences between healthy and unhealthy physical status in 16 of the 34 unhealthy physical status, including in patients with hypertension ($P=0$) and gout ($P=6.48\times10^{-90}$). Exercise habits (E-habits) showed 19 differences between healthy and unhealthy status, including in hyperlipidemia ($P=1.28\times10^{-277}$) and diabetes ($P=4.20\times10^{-29}$). Dietary habits also showed differences in 10 unhealthy status, including in chronic pharyngitis ($P=2.59\times10^{-19}$) and cholecystolithiasis ($P=9.43\times10^{-18}$). We detected differences for alcohol intake habits in 20 unhealthy status, including hyperlipidemia ($P=0$), coronary heart disease ($P=4.06\times10^{-24}$), diabetes ($P=1.09\times10^{-22}$) and Parkinson's syndrome ($P=1.43\times10^{-17}$). We also observed differences for smoking habits in 18 unhealthy status when compared to the unhealthy condition, including in hypertension ($P=2.74\times10^{-114}$), hyperlipidemia ($P=2.69\times10^{-62}$) and Parkinson's syndrome ($P=5.12\times10^{-29}$). We found differences for IOP-R in five unhealthy status compared with healthy, including in hypertension ($P=3.63\times10^{-85}$) and diabetes ($P=2.01\times10^{-73}$); similar findings were produced for IOP-L (Fig. 4, Supplementary Table 36). For lipids PEIs, we also observed differences between 34 unhealthy and healthy status. For example, LDL-C was detected in 21 unhealthy status, including hypertension ($P=0$) and diabetes ($P=2.95\times10^{-212}$). HDL-C was detected in 17 unhealthy status, including in diabetes ($P=1.92\times10^{-177}$) (Fig. 4, Supplementary Table 36). We further conducted a detailed analysis of HDL-C and diabetes and found those with low HDL-C showed a significantly higher risk of developing diabetes than those with average values (1.26-1.75 mmol/L) in this population. Of note, those with high HDL-C levels also showed elevated risk of developing diabetes (Extended data Fig. 2).

Tumor-associated antigens also display significant differences between the healthy and unhealthy status. For example, CYFRA 21-1 was detected in 10 unhealthy status, including hypertension+diabetes (P=3.71×10$^{-97)}$ and diabetes (P=4.52×10^{-70}). CEA1 was detected in 12 unhealthy status, including hypertension+coronary (P=9.59×10^{-29}) and diabetes (P=1.73×10^{-18}). Alpha-fetoprotein (AFP) was detected in hepatopathy (P=1.08×10^{-28}). C-PSA was detected in hypertension+coronary (P=8.38×10^{-20}). Finally, the carbohydrate antigen CA724 (CA 72-4) was detected in asthma (P=9.92×10^{-13}), gout (P=3.53×10^{-7}) and coronary+diabetes (P=4.06×10^{-5}) (Fig. 4, Supplementary Table 36). Among other PEIs, we also detected significant differences between the healthy and unhealthy status. For example, we found differences in urine sugar levels (U-GLU) in nine unhealthy status, including in diabetes and its associated diseases. The eosinophil rate (eo%), was found in five unhealthy status, including asthma (P=1.38×10^{-129}) and rhinallergosis (P=4.05×10^{-18}). Whole blood iron levels (WB-Fe) was found in 11 unhealthy status, including hypertension (P=2.52×10^{-69}). We detected PH in 11 unhealthy status, including diabetes (P=1.97×10^{-239}), hypertension (P=2.41×10^{-166}), hypertension+diabetes (P=9.90×10^{-32}) and gout (P=9.82×10^{-15}). We found potassium (K+) in five unhealthy status, including hypertension (P=1.98×10^{-119}) and hepatitis B (P=3.13×10^{-10}). We also detected differences in magnesium (Mg2+) in hypertension+diabetes (P=3.14×10^{-58}) and diabetes (P=5.10×10^{-52}). Hcy (an indicator of cardiovascular disease) was detected in eight unhealthy status, including hypertension (P=1.97×10^{-136}) and Parkinson's syndrome (P=1.76×10^{-7}) (Fig. 4, Supplementary Table 36). These results provide a set of candidate markers for chronic diseases early diagnosis.

Machine learning to predict healthy and unhealthy physical status from PEIs

A key objective of this study was to apply PEI data and machine learning technology to develop algorithms that can predict the onset of common disease based on general physical examination. We tried three machine learning models, including kernelized support vector machine (SVM), multilayer perceptron (MLP) and random forests. Because SVM and MLP prediction models only gave very low accuracy and sensitivity in our initial training data, we excluded these models for further training. Random forests showed better performance than SVM and MLP in the initial training. However, it could not give good performance in the multi-class classification of all the physical status. Finally, we

tried to use binary classification to classify each pair of healthy and unhealthy physical status (e.g. hypertension and healthy people; Parkinson's syndrome and healthy people) and we obtained relatively better performance than the multi-class classification. Then we tried to optimize this prediction algorithm. Because the data were characterized by serious category imbalance, a random under-sampling method, was adopted that balances the data by randomly selecting the data subset of the target class. In each physical status, the top 15% or 16% representative PEIs were extracted for prediction by feature extraction. The advantage of this method is that it is usually very fast and completely independent of the model applied after feature selection.

Finally, in the random forests algorithm prediction of each pair of healthy and unhealthy physical status, the area under curve (AUC) of receiver operating characteristic curve reached 66%~99% depending on the unhealthy physical status (average 87.6%) (Fig.5, Extended data Table 2, Extended data Table 3 and Supplementary Table 37). For classification, AUC values more than 90% indicated excellent performance, and values from 80% to 90% indicated good performance. Our algorithm provided high-precision predictions in 18 of the 34 unhealthy physical status (AUC>90%), good performance for another 9 of the unhealthy physical status (90% >AUC>80%). In our algorithm, patients with heart-related diseases showed excellent performance. For example, by extraction 30 PEI features (age, leukocyte count, monocytes, Mon%, mean corpuscular volume, red blood cell count, red cell distribution width, lymphocyte rate, platelet count, low-density lipoprotein, high-density lipoprotein, total cholesterol, carcinoembryonic antigen 1, albumin, albumin-globulin, cystatin c, glucose, urine sugar, urine creatinine, estimated glomerular filtration rate, creatinine, urea, waistline, aaist-hip Ratio, body mass index, operation history, systolic pressure, height, neck size and anamnesis, Extended data Table 2), Hypertensive+Diabetes+Coronary Heart Disease provides 99% AUC just using 909 training samples and 387 validation samples (f1-score (95%CI), 0.96(0.95-0.96); accuracy (95%CI): 0.95(0.94-0.97); specificity (95%CI): 0.95(0.94-0.95); recall (sensitivity) (95%CI): 0.95(0.94-0.97). In our algorithm, patients with Parkinson's syndrome provides 97% AUC using 192 training samples and 83 validation samples (f1-score (95%CI), 0.91(0.90-0.91); accuracy (95%CI): 0.90(0.89-0.90); specificity (95%CI): 0.87(0.79-0.94); recall (95%CI): 0.90(0.89-0.91). For hepatic adipose infiltration, our algorithm also provided good prediction performance using 803 training samples and 115 validation samples (f1-score (95%CI), 0.82(0.78-0.87); accuracy (95%CI): 0.81(0.76-0.86) ;

specificity (95% CI): 0.75(0.67-0.82); recall (95% CI): 0.82(0.77-0.87) and AUC (95% CI): 0.92(0.89-0.94). For chronic rhinitis, we got the lowest prediction performance in this study (AUC(95%CI):0.66(0.60-0.72)). When all unhealthy physical status were classified as one "unhealthy" status together, our algorithm also provided good predictions: f1-score (95%CI): 0.83 (0.83-0.83); accuracy (95%CI): 0.82 (0.82-0.82); specificity (95%CI): 0.81(0.81-0.81); sensitivity (95%CI): 0.84 (0.84-0.84) and AUC (95%CI): 0.9 (0.90-0.90). These results suggested that by using feature extraction of the PEIs (15-16% of all 221 PEIs) just by using small number of samples, our random forests algorithms provided good performance for majority unhealthy physical status predictions.

Discussion

This study has produced correlation maps of 221 routine PEIs using physical examination data obtained from a Chinese population of 803,614 individuals of 35 healthy or unhealthy physical status (mainly chronic diseases). We detected a large number of correlations among PEIs in healthy or unhealthy physical states; furthermore, these correlations differed according to the 34 unhealthy physical conditions analyzed. Most of the correlations are newly observed in this study. We found that a wide range of correlations among PEIs, such as sex, age, BMI, blood lipids, blood pressures, cancer-related indicators, lifestyles including drinking, smoking, e-habits. Improving our understanding these PEI interactions will help explain disease mechanisms and pathogenesis. Our results fill the gap of systematic PEI analysis and provide rich information about how PEIs might reflect underlying health conditions. These findings provide rich information to further improve healthcare researches and clinical practice.

One of the unexpected finding from our analysis was that patients with hypertension showed more correlations between HBV-DNA and HCV-RNA to other PEIs than healthy cohort. Similarly, we found a strong correlation between hepatitis C virus and other PEIs in diabetes, suggesting that patients infected with hepatitis C may be more susceptible to diabetes. This finding implicates a phenomenon whereby viral infection can make an individual more susceptible to developing a chronic disease. For these people, antiviral therapy might be taken into consideration while treating hypertension and diabetes.

Biomarker discovery and development for clinical research, diagnostics and therapy monitoring in clinical trials are key areas of medicine and healthcare[6]. In this study, we presented many candidate markers for chronic disease. For example, we found that IOP indicators, which are considered to be a relatively independent marker for glaucoma[20], are closely associated to hypertension, diabetes, and hypertension with diabetes. These results suggest that IOP might be affected, to some extent, by systemic diseases and might be used as one of the clinical marker of these diseases early diagnosis. Our results confirmed that low HDL-C level is a risk factor for diabetes[21], especially in women. This result suggests that improving HDL-C level through dietary supplementation might be an effective way to prevent diabetes in patients with low HDL-C levels. However, based on our results, excessive HDL-C supplementation is also a risk factor; therefore, HDL-C supplementation should aim to bring HDL-C levels within a normal range[22]. We detected a significant increase in AFP in hepatopathy when comparing healthy cohort, which confirms AFP increase is an increased risk factor for primary liver cancer in hepatopathy[14-15]. K^+ has significant effects on hypertension[23] and Cl^-, and Mg^{2+} has significant effects on diabetes, suggesting that modulation of these ions might have effects on these conditions. Living habits, such as exercise, smoking and drinking, have a more profound impact on the body than we had expected. For example, exercise, drinking or smoking history have a strong impact on hyperlipidemia[24-25], as evidenced by comparision to healthy status. This finding suggests that by adjusting these living habits, hyperlipidemia should improve.

Because the current physical examination conclusion is generally based on a relatively independent single or several prior indicators to give advice on the results of physical examination, many of the results given are ambiguous, and the value of judging the health status of the examinees is very limited[10,26-27]. There is an urgent need for a more accurate index system and method to judge the health status of physical examinees. In the final part of our study, we developed random forest machine learning algorithms that can predict diseases through 15%-16% of all 221 PEIs with good performance of prediction (AUC:66%~99%; average 86%). For each disease, we defined about 30 contributed PEIs by feature extraction. In most of our prediction algorithms, only a few hundreds of samples were needed to give good prediction performance for many chronic diseases. This finding suggests machine learning on PEI data can be used to help predict the true condition of the examers, identify “at-risk” patients and indicate the most relevant follow-up physical examinations for affected individuals.

In summary, we systematically explored the correlation between various PEIs and their relationship with chronic diseases and established machine learning prediction models to predict health status. This study provides abundant information to better understand the physiological and pathological characteristics of the human body as a system. Importantly, we have identified modifiable factors and directions for disease prediction, diagnosis and treatment. Our developed machine learning algorithms can be immediately applied to clinical practice to assistant the judgment of physical examination results.

Methods

Study approval

The study was approved by the institutional ethics committee of Sichuan Provincial People's Hospital and was conducted according to the Declaration of Helsinki principles. Informed consent was obtained from the participants when possible.

Study Participants

PEI data were obtained from 803,614 Han Chinese patients visiting the Health Management Center & Physical Examination Center of Sichuan Provincial People's Hospital in China between 2013 and 2018. The total cohort captured participants with 35 different reported health conditions, including 711,928 reported healthy participants and 91,686 unhealthy participants. The unhealthy cohort included 46,981 patients with hypertension, 11,745 with diabetes and 32,960 with other unhealthy status (Table 1).

Detected PEIs

Only the PEIs that were recorded by the same methods were included in this study. In total, 229 PEIs were initially collected: eight PEIs that were detected in few individuals were excluded, leaving 221 PEIs for further analysis (Extended data Table 1). These PEIs included the levels of biochemical indicators and the results of blood tests. Patient lifestyles and disease conditions were also investigated during the physical examination.

Data processing

The PEIs with string variables were converted to integer variables for data analysis. Categorized variables were digitally coded for further calculation. The mean value imputation method was used for missing data. For individuals who participated in more than one physical check, average values of each PEI were used for data analysis.

Statistical Analyses

The Pearson correlation coefficient (PCC) method was used to calculate the correlations between two PEIs (for example, x and y) in R; this method measures the linear dependence between two variables. PCC correlation (r) (1) and *P* values (2) were calculated using the following formulae[28-30]:

(1)

$$r = \frac{n(\sum xy) - (\sum x)(\sum y)}{\sqrt{[n\sum x^2 - (\sum x)^2][n\sum y^2 - (\sum y)^2]}}$$

(2) $P = 1 - F.DIST(((n-2)*r^2)/(1-r^2), 1, n-2)$

df = n - 2

n = number of x-y data pairs

Total sample size required when using the correlation coefficient (r), when two-sieded α=0.05, β=0.20. If r=0.05, we need 3,134 samples; if r=0.10, we need 782 samples; if r=0.25, we need 123 samples; if r=0.5, we need 29 samples. The general formula for the correlation sample calculating is listed as the following (3)[31]:

(3) r = expected correlation coefficient

$C = 0.5 \times \ln [(1 + r)/(1 - r)]$

N = Total number of subjects required

Then

$N = [(Z_\alpha + Z_\beta) \div C]2 + 3.$

A linear regression model (lm) was used to compare PEIs between the reported healthy status and unhealthy status adjusted for sex and age in the R package[21-23]. The odds ratio of HDL-C level was calculated by using generalized linear models (glm) adjusted for age in the R package[24-25]. The correlation interaction network was conducted using qgraph[10-11].

Machine learning

Three machine learning models, including kernelized support vector machine (SVM)[28-29], multilayer perceptron (MLP)[30-32] and random forest[33] were tested to get the prediction performance of the PEIs. By using MLP algorithm prediction in neural network to predict health and each of the 34 unhealthy status (multi classification), it could not achieve good results. We further tried prediction the healthy from each unhealthy statues by the binary classification method, the F1 value of the prediction each

result is very close to zero. By using SVM algorithm prediction for making multi classification prediction, the highest F1 value of cholecystolithias is 0.70, but that of most other types of diseases is 0.00. We also tried the binary classification method, but all the results were relatively poor. When random forest algorithm is used for prediction for multi classification (health and each of the 34 unhealthy status), the F1 value of healthy status can reach 0.80-0.90, but the F1 value of unhealthy sattus is about 0.00-0.40. Then, we further chosen forest algorithm and optimized the random forest algorithm. First, due to the uneven distribution of the sample numbers of healthy and non-healthy status, and the law of large numbers[32], we used downsampling strategy for sample randomly used. Because the data were characterized by serious category imbalance, a random under-sampling method, was adopted that balances the data by randomly selecting the data subset of the target class. Second, we used PEI feature extraction strategy to extract the most contributed PEI for each healthy and unhealthy status. Feature extraction adopts the strategy of univariate statistics in automatic feature selection. Univariate statistics select features with high confidence according to the statistical significance of the relationship between each feature and the target. This process can be achieved by using feature_selection in scikit-learn. Finally, in each healthy and non-healthy status, the top 15% or 16% representative PEIs were extracted for prediction by feature extraction. The advantage of this method is that it is usually very fast and completely independent of the model applied after feature selection. Then, the data were randomly divided such that 30% constituted the test set, and the remaining 70% were randomly divided again, with 70% as the training set for the training model and 30% as the validation set for the evaluation model. In the process of improving the generalization performance of the model by adjusting parameters, a cross-validation method with a grid search was adopted, which can be implemented by GridSearchCV provided by scikit-learn (Supplementary Table 37 and Supplementary code).

References

1 Steenhuis, S., Groeneweg, N., Koolman, X. & Portrait, F. Good, better, best? A comprehensive comparison of healthcare providers' performance: An application to physiotherapy practices in primary care. *Health Policy* **121**, 1225-1232, doi:S0168-8510(17)30274-9 [pii], 10.1016/j.healthpol.2017.09.021 (2017).

2 Liu, Q., Tian, X., Tian, J. & Zhang, X. Evaluation of the effects of comprehensive reform on primary healthcare institutions in Anhui Province. *BMC Health Serv Res* **14**, 268, doi:1472-6963-14-268 [pii, 10.1186/1472-6963-14-268 (2014).

3 Perry, H. B., Shanklin, D. S. & Schroeder, D. G. Impact of a community-based comprehensive primary healthcare programme on infant and child mortality in Bolivia. *J Health Popul Nutr* **21**, 383-395 (2003).

4 Lennox, N. G., Green, M., Diggens, J. & Ugoni, A. Audit and comprehensive health assessment programme in the primary healthcare of adults with intellectual disability: a pilot study. *J Intellect Disabil Res* **45**, 226-232, doi:jir303 [pii] (2001).

5 Mills, A. Health care systems in low- and middle-income countries. *The New England journal of medicine* **370**, 552-557, doi:10.1056/NEJMra1110897 (2014).

6 Keenan, G. M. Big Data in Health Care: An Urgent Mandate to CHANGE Nursing EHRs! *On-line journal of nursing informatics* **18** (2014).

7 van Ginneken, E. Perennial Health Care Reform--The Long Dutch Quest for Cost Control and Quality Improvement. *The New England journal of medicine* **373**, 885-889, doi:10.1056/NEJMp1410422 (2015).

8 Krogsboll, L. T., Jorgensen, K. J. & Gotzsche, P. C. General health checks in adults for reducing morbidity and mortality from disease. *The Cochrane database of systematic reviews* **1**, CD009009 (2019).

9 Frieden, T. R. SHATTUCK LECTURE: The Future of Public Health. *The New England journal of medicine* **373**, 1748-1754, doi:10.1056/NEJMsa1511248 (2015).

10 Goroll, A. H. Toward Trusting Therapeutic Relationships--In Favor of the Annual Physical. *The New England journal of medicine* **373**, 1487-1489, doi:10.1056/NEJMp1508270 (2015).

11 Krogsboll, L. T., Jorgensen, K. J., Gronhoj Larsen, C. & Gotzsche, P. C. General health checks in adults for reducing morbidity and mortality from disease: Cochrane systematic review and meta-analysis. *Bmj* **345**, e7191, doi:10.1136/bmj.e7191 (2012).

12 Vigilante, K., Escaravage, S. & McConnell, M. Big Data and the Intelligence Community - Lessons for Health Care. *The New England journal of medicine* **380**, 1888-1890 (2019).

13 Anoushiravani, A. A., Patton, J., Sayeed, Z., El-Othmani, M. M. & Saleh, K. J. Big Data, Big Research: Implementing Population Health-Based Research Models and Integrating Care to Reduce Cost and Improve Outcomes. *The Orthopedic clinics of North America* **47**, 717-724, doi:10.1016/j.ocl.2016.05.008 (2016).

14 Obermeyer, Z. & Emanuel, E. J. Predicting the Future - Big Data, Machine Learning, and Clinical Medicine. *The New England journal of medicine* **375**, 1216-1219, doi:10.1056/NEJMp1606181 (2016).

15 Ngiam, K. Y. & Khor, I. W. Big data and machine learning algorithms for health-care

delivery. *The Lancet. Oncology* **20**, e262-e273, doi:10.1016/S1470-2045(19)30149-4 (2019).

16 Beam, A. L. & Kohane, I. S. Big Data and Machine Learning in Health Care. *Jama* **319**, 1317-1318 (2018).

17 Pazzani, M. J., Mani, S. & Shankle, W. R. Acceptance of rules generated by machine learning among medical experts. *Methods Inf Med* **40**, 380-385, doi:01050380 [pii] (2001).

18 Kononenko, I. Machine learning for medical diagnosis: history, state of the art and perspective. *Artif Intell Med* **23**, 89-109, doi:S0933-3657(01)00077-X [pii] (2001).

19 Yip, W. & Hsiao, W. Harnessing the privatisation of China's fragmented health-care delivery. *Lancet* **384**, 805-818, doi:S0140-6736(14)61120-X [pii], 10.1016/S0140-6736(14)61120-X (2014).

20 Sultan, M. B., Mansberger, S. L. & Lee, P. P. Understanding the importance of IOP variables in glaucoma: a systematic review. *Surv Ophthalmol* **54**, 643-662, doi:S0039-6257(09)00116-7 [pii], 10.1016/j.survophthal.2009.05.001 (2009).

21 Schmidt, M. I. *et al.* Identifying individuals at high risk for diabetes: The Atherosclerosis Risk in Communities study. *Diabetes Care* **28**, 2013-2018, doi:28/8/2013 [pii], 10.2337/diacare.28.8.2013 (2005).

22 Borggreve, S. E., De Vries, R. & Dullaart, R. P. Alterations in high-density lipoprotein metabolism and reverse cholesterol transport in insulin resistance and type 2 diabetes mellitus: role of lipolytic enzymes, lecithin:cholesterol acyltransferase and lipid transfer proteins. *Eur J Clin Invest* **33**, 1051-1069 (2003).

23 Diness, J. G. *et al.* Effects on atrial fibrillation in aged hypertensive rats by Ca(2+)-activated K(+) channel inhibition. *Hypertension* **57**, 1129-1135, doi:HYPERTENSIONAHA.111.170613 [pii], 10.1161/HYPERTENSIONAHA.111.170613 (2011).

24 Chanoine, P. & Spector, N. D. Hyperlipidemia, eating disorders, and smoking cessation. *Curr Opin Pediatr* **20**, 734-739, doi:10.1097/MOP.0b013e32831a6bed, 00008480-200812000-00021 [pii] (2008).

25 Saito, Y. Secondary hyperlipidemia due to obesity and alcohol drinking. *Nihon Naika Gakkai Zasshi* **81**, 1784-1787 (1992).

26 Mehrotra, A. & Prochazka, A. Improving Value in Health Care--Against the Annual Physical. *The New England journal of medicine* **373**, 1485-1487, doi:10.1056/NEJMp1507485 (2015).

27 Donabedian, A. Evaluating the quality of medical care. 1966. *Milbank Q* **83**, 691-729, doi:MILQ397 [pii],10.1111/j.1468-0009.2005.00397.x (2005).

28 Brown, B. W., Jr., Lucero, R. J. & Foss, A. B. A situation where the Pearson correlation coefficient leads to erroneous assessment of reliability. *J Clin Psychol* **18**, 95-97 (1962).

29 Haldar, P. *et al.* Cluster analysis and clinical asthma phenotypes. *Am J Respir Crit Care Med* **178**, 218-224 (2008).

30 Kew, M. Alpha-fetoprotein in primary liver cancer and other diseases. *Gut* **15**, 814-821 (1974).

31 Hulley S.B, C. S. R., Browner W.S, Grady D, Newman T.B. . Designing clinical research : an epidemiologic approach. 4th ed. . *Philadelphia, PA: Lippincott Williams & Wilkins; 2013.*

Appendix 6C, page 79. (2013).

32 Laurikkala, J. P., Kentala, E. L., Juhola, M. & Pyvkko, I. V. A novel machine learning program applied to discover otological diagnoses. *Scand Audiol Suppl*, 100-102 (2001).

ACKNOWLEDGMENTS

We thank all the participants in this study. This research project was supported by: the National Natural Science Foundation of China (81970839(L.H.), 81670895 (L.H.) and 81300802 (L.H.); the Department of Science and Technology of Sichuan Province, China (2015JQO057 (L.H.), 2017JQ0024 (L.H.), 2016HH0072 (L.H.) and 2013JY0195 (L.H.); the Department of Science and Technology of Sichuan Province, China (2017JZ0039 (P.S.). The author is especially indebted to Dr. Yabing Mei for taking time to make extensive comments.

AUTHOR CONTRIBUTIONS

L.H. designed the study. P.S., Y.L., L.J., J.Y., S.Z., Y.Y., L.W., D.L. and T.Y. enrolled all the participants. L.H., H.W. and P.S. performed the data analysis. Y.D., S.Z. and Y.Y., did the machine learning prediction models. L.H. wrote the manuscript. All of authors critically revised and provided final approval for this manuscript.

COMPETING FINANCIAL INTERESTS

The authors declare no competing interests related to this paper.

Table 1. Summary of the study samples, detected correlations and the different PEIs between healthy status and unhealthy states

Body status	Sample (N)	Age (Range)	Female %	Sig. Correlation (a)	Sig. Correlation % (b)	Different PEIs (c)
Normal condition	711928	41.4（4~105）	45.7	7662	31.5	-
Cholecystolithiasis	993	50.09（19~97）	47.8	1622	6.9	28
Hypertension	46981	62.0（20~102）	36.1	4413	18.3	112
Hypertension+Diabetes	8586	67.3（34~99）	67.1	3008	12.6	100
Hypertension+Coronary	2074	74.0(34~98)	40.4	1920	7.7	53
Hypertensive+Diabetes+Coronary	928	73.5(37~98)	35	2014	8.7	56
Hyperlipidemia	1722	65.0(29~96)	33	2256	9.5	51
Coronary heart disease	1325	68.7(27~93)	24.6	1925	8.3	36
Coronary+Diabetes	280	70(44~89)	20.4	1335	6.2	40
Rhinallergosis	156	39（18~92）	39.7	1278	6.1	12
Hypothyroidism	1661	46.7(16~94)	84.6	1703	7.1	33
Hyperthyroidism	767	45.2（15~89）	66.6	1234	5.2	16
Cervical spondylopathy	318	53.7（27~87）	48.7	1589	7	14
Rheumatoid arthritis	396	55.0（24~86）	74.7	1039	4.5	29
Chronic rhinitis	320	38.6（21~85）	30.6	969	4.5	8
Nephropathy	76	48.6（23~91）	42	1771	7.8	31
Diabetes	11745	59.3(14~96)	24.9	2972	12.3	91
Gout	2138	51.8（20~97）	2	1813	7.8	52
Parkinson's syndrome	197	70.4（40~92）	26.4	1659	8.1	28
Stomach trouble	1296	49.5（19~95）	39.2	1523	6.5	37
Chronic pharyngitis	782	40.2（18~90）	32.7	1487	6.2	14
Lumbar disc protrusion	385	56.8（25~91）	35.6	982	4.3	12
Hepatitis B	706	45.3（22~82）	22.8	1084	4.5	34
Hypertension+other diseases	2409	64.6（28~94）	38.1	1750	7.1	67

Coronary+others	101	69.3(36~92)	33.7	569	3.3	12
Diabetes+others	373	63（29~90）	26.8	1045	4.6	35
Bronchial disease	574	60.7（19~95）	33.2	1276	5.6	19
Other disease conditions	2777	51.4(17~100)	43.8	2066	8.5	38
Brain diseases	257	69.9（27~98）	29.5	1023	4.7	25
Hepatic adipose infiltration	274	44.1（21~77）	12.4	1139	5.3	36
Asthma	280	51.0（12~91）	57.9	1388	5.9	23
Other Cardiac diseases	344	60.0（26~90）	55.9	749	3.6	19
Heart disease	229	69.7（26~96）	42.6	698	3.5	28
Hepatopathy	180	51.6（25~83）	38.7	702	3.6	25
Pregnant	56	29.7(24~36)	100	1015	8.5	25

(a) Significant correlations, the number of correlations with *P* values calculated by PCC adjusted by all the correlations ($P<0.05/ 24{,}322$ PEI pairs$=2\times10^{-6}$).

(b) Significant correlation %, which is the percentage of significant correlations in all the correlation pairs.

Detailed information on the correlations described in (a-b) is provided in Supplementary Table 1-35.

(c) The number of PEIs was significantly different between normal physical status and nonnormal physical states ($P<0.05/34$ nonnormal states$=1.4\times10^{-3}$). A linear regression model (lm) was used to compare PEIs between normal physical status and nonnormal physical states adjusted for gender and age. Detailed information for this summary is provided in Supplementary Table 36.

Figure legends:

Figure 1. The PEI correlations detected in the healthy cohort. a, A correlation map of the top 50 correlated PEIs, each of which had >114 significant correlations with other PEIs (FDR<0.05). b, The number of statistically significant correlations detected in the healthy population of each PEI.

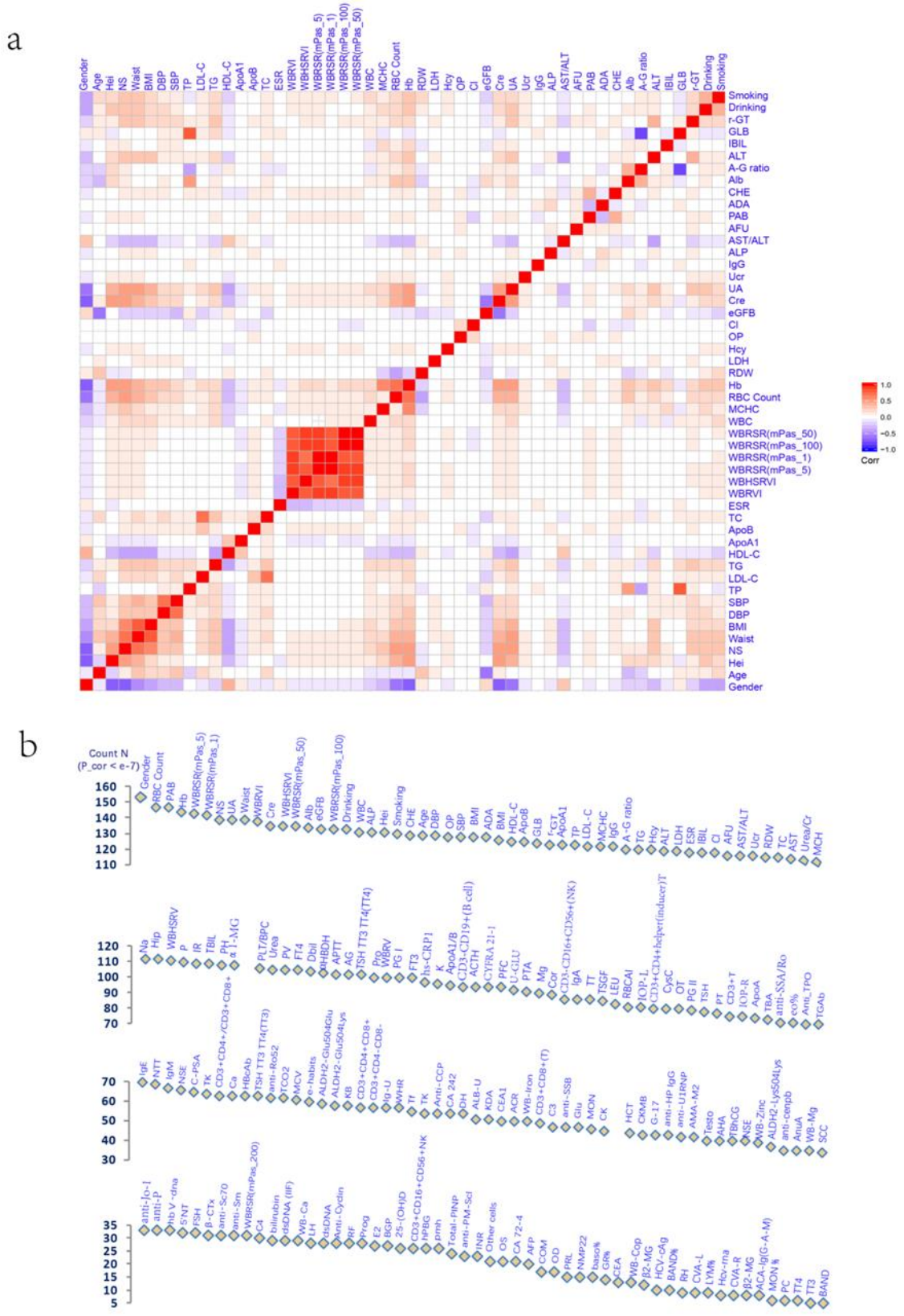

Figure 2. The correlation directions of typical PEIs in healthy physical conditions. The r values were calculated by the PCC method. See Extended data Table 1 for detailed PEI information.

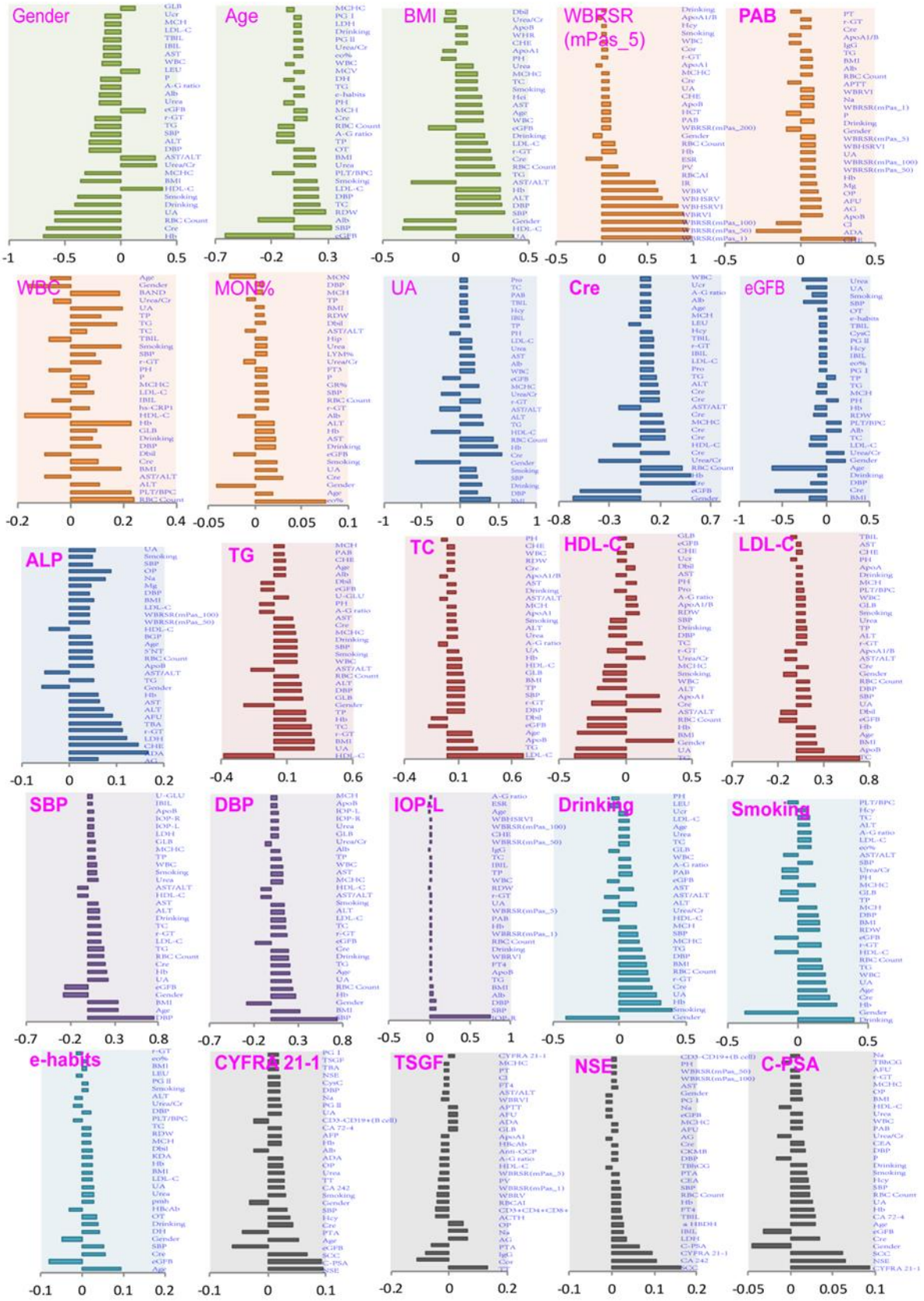

Figure 3. PEI networks in healthy physical status. In the weighted graphs, the green edges indicate positive weights, and the red edges indicate negative weights. The color saturation and the width of the edges correspond to the absolute weight and scale relative to the strongest weight in the graph, respectively. The circular layout shows how well the data conforms to the model while the force-oriented layout shows how each node (connected and unconnected) repulses the other, and how connected nodes attract each other. See also Supplementary Figures.

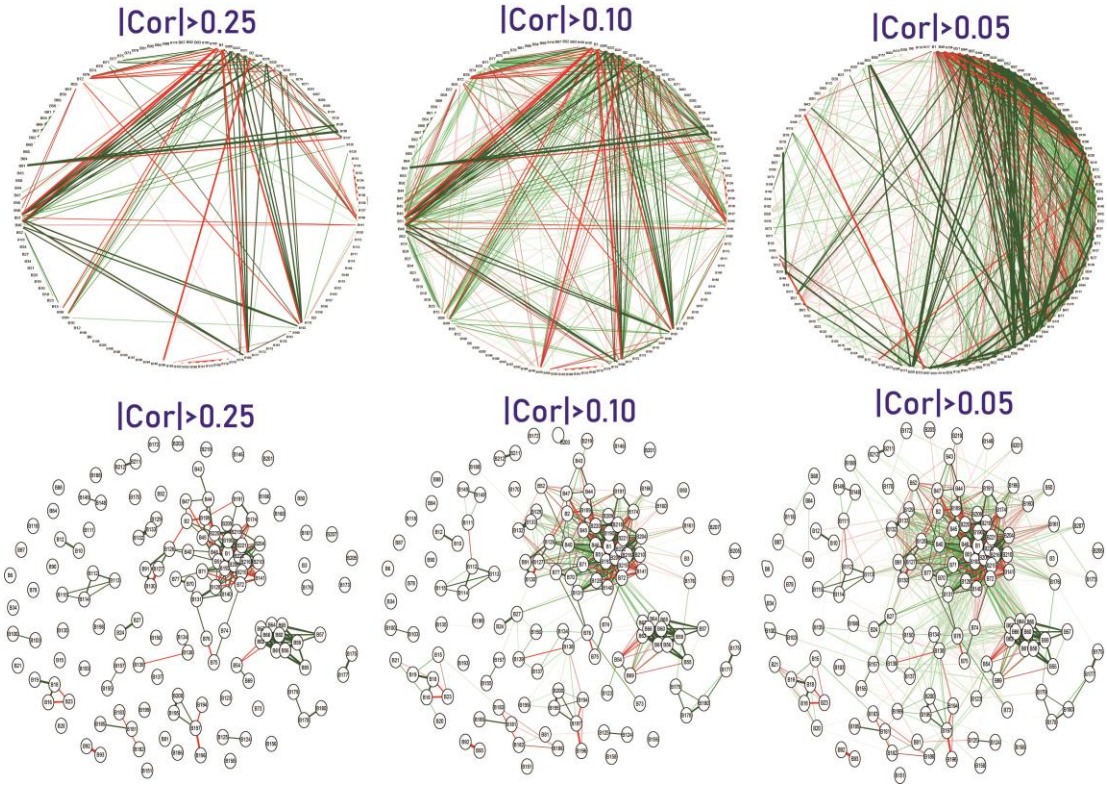

Figure 4. Representative candidate markers for unhealthy physical status. A linear regression model was used to compare PEIs between healthy physical states and unhealthy physical states after adjusting for sex and age. Significantly different PEIs (P <0.05) after Bonferroni adjustment (P<0.05/34 unhealthy states=1.4×10^{-3}) are shown. See also Supplementary Table 36.

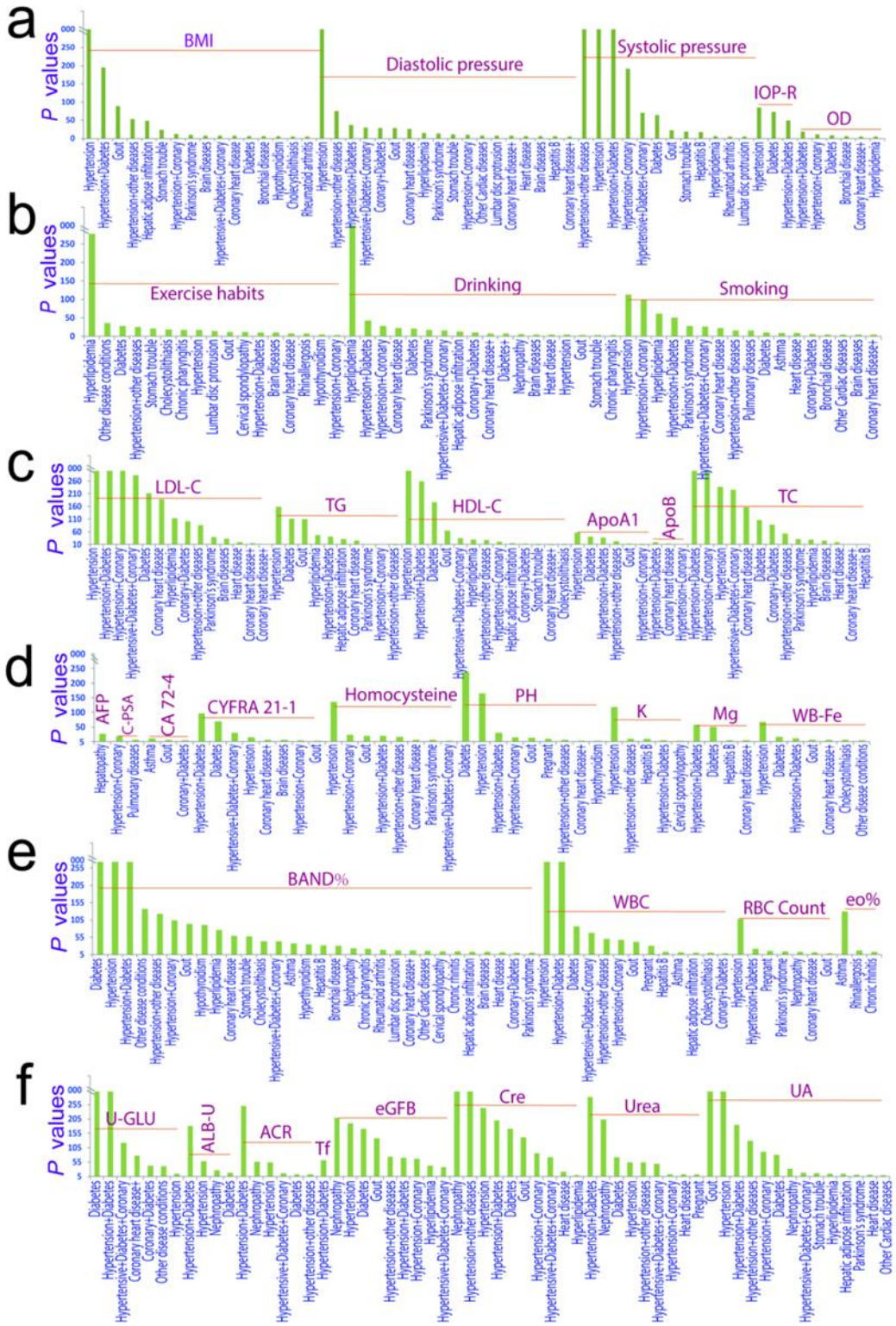

Figure 5. Machine learning prediction of the 35 physical status by the random forest algorism. The receiver operating characteristic curve takes the false positive rate (FPR) as the horizontal axis and the true positive rate (TPR) as the vertical axis. The horizontal axis represents the proportion of the actual negative instances in the positive class predicted by the classifier to all the negative instances, while the vertical axis represents the proportion of the actual positive instances in the positive class predicted by the classifier to all the positive instances. The AUC is the area under the ROC curve.

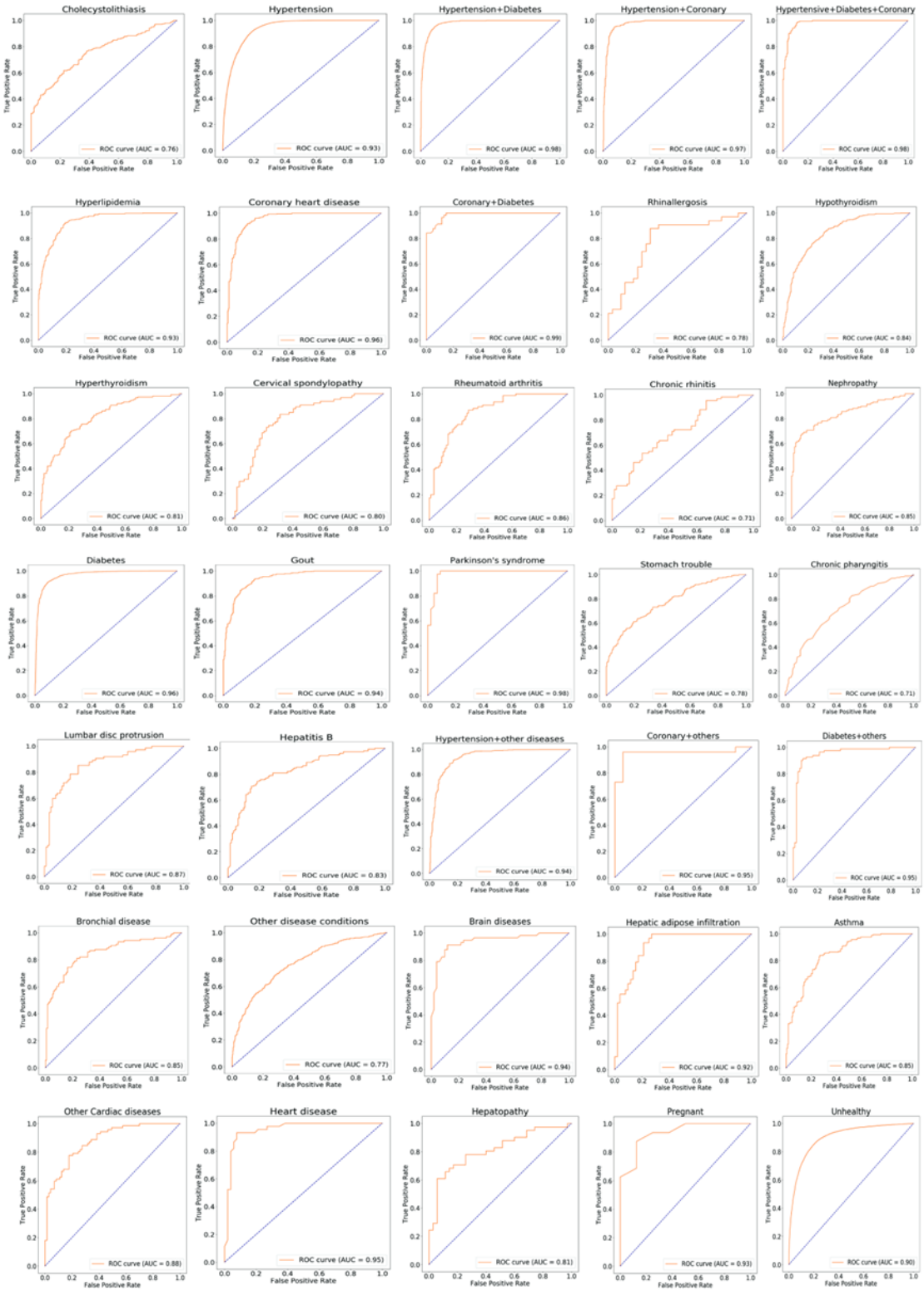

Extended data Table 1. PEIs used in this study

Code	PEI Name	PEI Name abbreviation	Unit
B1	Gender	Gender	-
B2	Age	Age	years
B3	Homocysteine	Hcy	umol/L
B4	Whole Blood Calcium	WB-Ca	mmol/L
B5	Whole Blood Magnesium	WB-Mg	mmol/L
B6	Iron Of Whole Blood	WB-Fe	mmol/L
B7	Whole Blood Copper	WB-Cop	umol/L
B8	Zinc In Whole Blood	WB-Zinc	umol/L
B9	Rh Blood Group	RH	-
B10	Pepsinogen I	PGI	ug/L
B11	PgI/PgII	PGI/PGII	-
B12	Pepsinogen II	PGII	ug/L
B14	Gastrin-17	G-17	pmol/l
B15	Cd3-Cd19+(B Cell)	CD3-CD19+(B cell)	-
B16	Cd3+ Total T Lymphocyte	CD3+T	-
B17	Cd3+Cd16+Cd56+Nk	CD3+CD16+CD56+NK	-
B18	Cd3+Cd4+Helper(Inducer)T Cells	CD3+CD4+helper(inducer)T	-
B19	Cd3+Cd4+/Cd3+Cd8+	CD3+CD4+/CD3+CD8+	-
B20	Cd3+Cd4+Cd8+	CD3+CD4+CD8+	-
B21	Cd3+Cd4-Cd8-	CD3+CD4-CD8-	-
B22	Cd3+Cd8+(T)	CD3+CD8+(T)	-
B23	Cd3-Cd16+Cd56+(Nk)	CD3-CD16+CD56+(NK)	-
B24	α Hydroxybutyrate Dehydrogenas	αHBDH	U/L
B25	Creatine Kinase	CK	U/L
B26	Creatine Kinase Isoenzyme	CKMB	U/L
B27	Lactic Dehydrogenase	LDH	U/L
B28	Pituitary Prolactin	PRL	mIU/L
B29	Estradiol E2	E2	pmol/L
B30	Luteinizing Hormone	LH	mIU/ml
B31	Follicle Stimulating Hormone	FSH	mIU/ml
B32	Testosterone	Testo	nmol/L
B33	Progesterone	Prog	nmol/L
B34	Thymidine Kinase	TK	PM/L
B35	Blood Beta-Microglobulin	β2-MG	-
B36	Variant Lymphocyte Rate	V-Lym%	-
B37	Band Cell	BAND	10E-9/L
B38	Band Cell%	BAND%	-
B39	Other Cell Types	Other cells	-
B40	Leukocyte Count	WBC	10E-9/L
B41	Monocytes	MON	-

B42	Monocytes %	MON %	10E-9/L
B43	Mean Corpuscular Volume	MCV	fl
B44	Mean Corpuscular Hemoglobin	MCH	pg
B45	Mean Corpuscular Hemoglobin Concentration	MCHC	g/l
B46	Red Blood Cell Count	RBC Count	10E-12/L
B47	Red Cell Distribution Width	RDW	fl
B48	Lymphocyte Rate	LYM%	-
B49	Basophilic Granulocyte Rate	baso%	-
B50	Eosinophil Rate	eo%	-
B51	Hemoglobin	Hb	g/L
B52	Platelet Count	PLT/BPC	10E-9/L
B53	Granulocyte Rate	GR%	-
B54	Erythrocyte Sedimentation Rate	ESR	mm/60min
B55	Erythrocyte Deformation Index	TK	-
B56	The Index Of Rigidity Of Erythrocyte	IR	-
B57	Erythrocyte Aggregation Indices	RBCAI	-
B58	Hematocrit	HCT	-
B59	Whole Blood Reduced Viscosity	WBRV	-
B60	Whole Blood Reduced Viscosity Index	WBRVI	-
B61	Whole Blood High Shear Reduced Viscosity	WBHSRV	-
B62	Whole Blood High Shear Reduced Viscosity Index	WBHSRVI	-
B63	Shear Rate Of Whole Blood Viscosity_Mpas_1 (200)	WBRSR(mPas_200)	-
B64	Shear Rate Of Whole Blood Viscosity_Mpas_3 (5)	WBRSR(mPas_5)	-
B65	Shear Rate Of Whole Blood Viscosity_Mpas_4 (1)	WBRSR(mPas_1)	-
B66	Shear Rate Of Whole Blood Viscosity_Mpas (100)	WBRSR(mPas_100)	-
B67	Shear Rate Of Whole Blood Viscosity_Mpas (50)	WBRSR(mPas_50)	-
B69	Plasma Viscosity	PV	-
B70	Low-Density Lipoprotein	LDL-C	mmol/L
B71	Triglyceride	TG	mmol/L
B72	High-Density Lipoprotein	HDL-C	mmol/L
B73	Apolipoprotein A	ApoA	mg/L
B74	Apolipoprotein A1	ApoA1	g/L
B75	Apolipoprotein A1/B	ApoA1/B	g/L
B76	Apolipoprotein B	ApoB	g/L
B77	Total Cholesterol	TC	mmol/L
B78	Hepatitis B Virus Core Im Antibod	HBcAb	-
B79	Quantitative Detection Of Hepatitis B Virus Dna	hbV-dna	IU/ml
B80	Helicobacter Pylori Antibody-Igg	anti-HP IgG	-
B81	Tumor Supplied Group Of Factors	TSGF	U/ML
B82	Carcinoembryonic Antigen	CEA	ng/ml
B83	Alpha-Fetoprotein	AFP	ng/ml
B84	Complexed Prostate Special Antigen	C-PSA	ng/ml
B85	Squamous Cell Carcinoma Antigen	SCC	ng/ml
B86	Chorionic Gonadotropin	TBhCG	mIU/ml

B87	Neuron-Specific Enolase	NSE	ng/ml
B88	Carbohydrate Antigen，Ca242	CA 242	U/ml
B89	Carbohydrate Antigen，Ca72_4	CA 72-4	U/ml
B90	Cytokeratin-19-Fragment Cyfra21-1	CYFRA 21-1	ng/ml
B91	Total Protein	TP	g/L
B92	Aldh2-Glu504Glu	ALDH2-Glu504Glu	-
B93	Aldh2-Glu504Lys	ALDH2-Glu504Lys	-
B94	Aldh2-Lys504Lys	ALDH2-Lys504Lys	-
B95	Anti-Cenpb	anti-cenpb	-
B96	Dsdna (Iif)	dsDNA (IIF)	-
B97	Anti-Dsdna Antibody	dsDNA	-
B98	Jo-1 Antibody	anti-Jo-1	-
B99	Anti-Pm-Scl	anti-PM-Scl	-
B100	Anti-Ro52	anti-Ro52	-
B101	Anti-Sc70	anti-Sc70	-
B102	Anti Sm Antibody	anti-Sm	-
B103	Anti-Ssa/Ro Antibody	anti-SSA/Ro	-
B104	Anti Ssb Antibody	anti-SSB	-
B105	Anti-U1Rnp Antibody	anti-U1RNP	-
B106	Anti-Ribosomal P Protein Antibody	anti-P	-
B107	Anti-Nucleosome Antibody Systemic	AnuA	-
B108	Anti-Cyclin Antibody	Anti-Cyclin	-
B109	Antimitochondrial Antibody M2	AMA-M2	-
B110	Anti-Histone Antibody	AHA	-
B111	Thyroid-Stimulating Hormon	TSH	mIU/L
B112	Free Thyroxine	FT4	pmol/L
B113	Free Triiodothyronine	FT3	pmol/L
B114	Total Thyroxine	TSH TT3 TT4(TT4)	nmol/L
B115	Total Triiodothyronine	TSH TT3 TT4(TT3)	nmol/L
B116	Total Triiodothyronine	TT3	nmol/L
B117	Total Thyroxine	TT4	nmol/L
B118	Carcinoembryonic Antigen 1	CEA1	ng/ml
B119	Quantitative Detection Of Hepatitis C Virus Rna	Hcv-rna	-
B120	Hcv Core Antigen	HCV-cAg	-
B121	Complement C3	C3	-
B122	Complement C4	C4	-
B123	High Sensitivity C-Reactive Protein 1	hs-CRP1	mg/L
B124	Adrenocorticotropic Hormone	ACTH	pg/ml
B125	Cortisol	Cor	ug/dl
B126	Albumin	Alb	g/L
B127	Albumin-Globulin	A-G ratio	-
B128	Alanine Aminotransferase	ALT	U/L
B129	Indirect Bilirubin	IBIL	umol/L
B130	Globulin	GLB	g/L

B131	Aspartate Transaminase	AST	U/L
B132	Direct Bilirubin	Dbil	umol/L
B133	Total Bilirubin	TBIL	umol/L
B134	Cholinesterases	CHE	KU/L
B135	Total Bile Acid	TBA	umol/L
B136	5-Nucleotidase	5'NT	U/L
B137	Alpha-L-Fucosidase	AFU	U/L
B138	Prealbumin	PAB	mg/L
B139	Adenosine Deaminase	ADA	U/L
B140	R-Glutamyl Transpeptidase	r-GT	U/L
B141	Ast/Alt	AST/ALT	-
B142	25-Hydroxyvitamin D	25-(OH)D	ng/mL
B143	β-Crosslaps	β-CTx	pg/mL
B144	Total-Pinp	Total-PINP	ng/mL
B145	Osteocalcin	BGP	ng/mL
B146	Cystatin C	CysC	mg/L
B148	Antithyroperoxidase Antibody	Anti_TPO	IU/ml
B149	Anti-Thyroglobulin Antibodies	TGAb	IU/ml
B150	Alkaline Phosphatase	ALP	U/L
B151	Anti-Cyclic Peptide Containing Citrulline	Anti-CCP	Ru/ml
B152	Anti Cardiolipin Antibodyig(G-A-M)	ACA-Ig(G-A-M)	u/ml
B153	Glucose	Glu	mmol/L
B154	Rheumatoid Factor	RF	IU/ml
B155	Immunoglobulin A	IgA	g/l
B156	Immunoglobulin E	IgE	IU/ml
B157	Immunoglobulin G	IgG	g/l
B158	Immunoglobulin M	IgM	g/l
B159	Urine Beta-Microglobulin	β2-MG	-
B160	Ph	PH	-
B161	Leucocyte	LEU	/ul
B163	Specific Gravity	SG	-
B164	Calcium Oxalate Crystals	COM	HPF
B165	Bilirubin	bilirubin	-
B166	Protein	Pro	-
B167	Phosphate Crystals	PC	-
B168	Urinary Nuclear Matrix Protein 22	NMP22	-
B169	Urate Crystal	U-CRY	-
B170	Urine Sugar	U-GLU	-
B171	Epithelial Cell	EC	HPF
B172	Ketone Body	KB	-
B173	Nitrous Acid	NTT	-
B174	Urea Creatinine	Urea/Cr	-
B175	Microalbuminuria	ALB-U	mg/L
B176	Urine Creatinine	Ucr	umol/L

B177	Ratio Of Urinary Microalbumin To Creatinin	ACR	ug/mg
B178	Urinary Immunoglobulin G	Ig-U	mg/L
B179	Urine Alpha-Microglobulin	α1-MG	mg/L
B180	Urine Transferrin	Tf	mg/L
B181	Activated Partial Thromboplastin Time	APTT	s
B182	Thrombin Time	TT	s
B183	Percentage Activity Of Prothrombin In Plasma	PTA	-
B184	International Normalized Ratio	INR	-
B185	Prothrombin Time	PT	s
B186	Plasma Fibrinogen Concentration	PFC	g/l
B187	Neuron-Specific Enolase	NSE	ng/ml
B188	Calcium	Ca	mmol/L
B189	Estimated Glomerular Filtration Rate	eGFB	ml/min
B190	Creatinine	Cre	umol/L
B191	Urea	Urea	mmol/L
B192	Uric Acid	UA	umol/L
B193	Kalium	K	mmol/L
B194	Chlorine	Cl	mmol/L
B195	Sodium	Na	mmol/L
B196	Blood Carbon Dioxide	TCO2	mmol/L
B197	Anion Gap	AG	mmol/L
B198	Phosphorus	P	mmol/L
B199	Magnesium	Mg	mmol/L
B200	Osmotic Pressure	OP	mOsm/L
B201	Exercise Habits	e-habits	-
B202	Frequency Of Exercises	e-times	-
B203	Dietary Habits 1	DH	-
B204	History Of Alcohol Intake	Drinking	-
B205	Known Of Drug Allergy	KDA	-
B206	Waistline	Waist	cm
B207	Waist-Hip Ratio	WHR	-
B209	Smoking History	Smoking	-
B210	Hipline	Hip	cm
B211	Intra-Ocular Tension Of The Right Eye	IOP-R	mmHg
B212	Intra-Ocular Tension Of The Left Eye	IOP-L	mmHg
B213	Corrected Visual Acuity The Right Eye	CVA-R	-
B214	Corrected Visual Acuity The Left Eye	CVA-L	-
B215	Body Mass Index	BMI	-
B216	Body Mass	BMI	kg
B218	Diastolic Pressure	DBP	mmHg
B219	Operation History	OT	-
B220	Systolic Pressure	SBP	mmHg
B221	Height	Hei	cm
B222	Neck Size	NS	cm

B223	Family History	FH	-
B224	Anamnesis	pmh	-
B225	Hourly Postprandial Blood Sugar	hPBG	mmol/L
B227	Vision Of The Right Eye	OD	-
B228	Vision Of The Left Eye	OS	-

Extended data Table 2. List of the 15% or 16% representative PEIs were extracted for machine learning prediction by feature extraction.

Healthy status	PEI features
Cholecystolithiasis	age, estimated glomerular filtration rate, systolic pressure, glucose, high-density lipoprotein, anamnesis, waistline, body mass index, exercise habits, neck size, hipline, low-density lipoprotein, urinary nuclear matrix protein 22, urine creatinine, thyroid-stimulating hormon, quantitative detection of hepatitis C virus RNA, specific gravity, dietary habits 1, pepsinogen II, osmotic pressure, creatine kinase isoenzyme, pepsinogen I, PH, anion gap, erythrocyte aggregation Indices, immunoglobulin A, osteocalcin, sodium, tumor supplied group of factors, whole blood reduced viscosity
Hypertension	age, estimated glomerular filtration rate, systolic pressure, glucose, high-density lipoprotein, waistline, body mass index, neck size, hipline, albumin, red cell distribution width, urea, monocytes, creatinine, height, diastolic pressure, uric acid, lymphocyte rate, cystatin c, albumin-globulin, operation history, body mass, monocytes %, waist-hip ratio, exercise habits, gender, smoking history, triglyceride, globulin, aspartate transaminase, lactic dehydrogenase, total cholesterol
Hypertension+Diabetes	age, estimated glomerular filtration rate, systolic pressure, glucose, high-density lipoprotein, waistline, body mass index, neck size, hipline, albumin, red cell distribution width, urea, monocytes, creatinine, height, diastolic pressure, uric acid, lymphocyte rate, cystatin c, albumin-globulin, operation history, body mass, monocytes %, waist-hip ratio, anamnesis, PH, platelet count, urine sugar, red blood cell count, hemoglobin, leukocyte count, urea creatinine
Hypertension+Coronary heart disease	age, albumin, albumin-globulin, anamnesis, body mass index, creatinine, cystatin c, direct bilirubin, estimated glomerular filtration rate, glucose, height, hemoglobin, known of drug allergy, lactic dehydrogenase, low-density lipoprotein, mean corpuscular volume, monocytes, monocytes %, neck size, operation history, platelet count, red blood cell count, red cell distribution width, specific gravity, systolic pressure, total cholesterol, urea, uric acid, waist-hip ratio, waistline
Hypertensive+Diabetes+Coronary Heart Disease	age, albumin, albumin-globulin, anamnesis, body mass index, creatinine, cystatin c, estimated glomerular filtration rate, glucose, height, low-density lipoprotein, mean corpuscular volume, monocytes, monocytes %, neck size, operation history, platelet count, red blood cell count, red cell distribution width, systolic pressure, total cholesterol, urea, waist-hip ratio, waistline, carcinoembryonic antigen 1, high-density lipoprotein, leukocyte count, lymphocyte rate, urine creatinine, urine sugar
Hyperlipidemia	age, albumin, anamnesis, body mass index, creatinine, estimated glomerular filtration rate, glucose, low-density lipoprotein, mean corpuscular volume, monocytes, neck size, operation history, platelet count, red blood cell count, red cell distribution width, systolic pressure, urea,

	waist-hip ratio, waistline, carcinoembryonic antigen 1, high-density lipoprotein, urine creatinine, known of drug allergy, specific gravity, uric acid, exercise habits, gender, history of alcohol intake, mean corpuscular hemoglobin, smoking history, total Protein, triglyceride
Coronary heart disease	age, albumin, anamnesis, body mass index, creatinine, estimated glomerular filtration rate, glucose, low-density lipoprotein, mean corpuscular volume, monocytes, neck size, operation history, platelet count, red blood cell count, red cell distribution width, systolic pressure, urea, waist-hip ratio, waistline, carcinoembryonic antigen 1, known of drug allergy, gender, mean corpuscular hemoglobin, total Protein, cystatin c, monocytes %, total cholesterol, direct bilirubin, lactic dehydrogenase, calcium, dietary habits 1, eosinophil rate
Coronary heart disease+Diabetes	age, albumin, anamnesis, body mass index, creatinine, estimated glomerular filtration rate, glucose, low-density lipoprotein, mean corpuscular volume, monocytes, neck size, operation history, platelet count, red blood cell count, red cell distribution width, systolic pressure, urea, waist-hip ratio, waistline, carcinoembryonic antigen 1, gender, mean corpuscular hemoglobin, monocytes %, total cholesterol, urine sugar, adenosine deaminase, alpha-l-fucosidase, CD3+CD16+CD56+NK, pepsinogen I, PH
Rhinallergosis	albumin, anamnesis, mean corpuscular volume, platelet count, waist-hip ratio, mean corpuscular hemoglobin, CD3+CD16+CD56+NK, known of drug allergy, total Protein, dietary habits 1, eosinophil rate, uric acid, exercise habits, triglyceride, 5-nucleotidase, alkaline phosphatase, AST/ALT, blood carbon dioxide, carcinoembryonic antigen, cholinesterases, erythrocyte sedimentation rate, free triiodothyronine, hematocrit, immunoglobulin M, Indirect bilirubin, total bilirubin, urinary nuclear matrix protein 22, vision of the left eye, vision of the right eye, whole blood high shear reduced viscosity index
Hypothyroidism	albumin, anamnesis, uric acid, AST/ALT, free triiodothyronine, age, creatinine, monocytes, neck size, red blood cell count, red cell distribution width, waistline, gender, monocytes %, high-density lipoprotein, specific gravity, history of alcohol intake, smoking history, albumin-globulin, height, leukocyte count, hemoglobin, alanine aminotransferase, anti-thyroglobulin antibodies, antithyroperoxidase antibody, body mass, diastolic pressure, mean corpuscular hemoglobin concentration, protein, r-glutamyl transpeptidase, thyroid-stimulating hormon, total Triiodothyronine, urea creatinine
Hyperthyroidism	albumin, anamnesis, age, creatinine, neck size, gender, high-density lipoprotein, specific gravity, history of alcohol intake, height, hemoglobin, anti-thyroglobulin antibodies, antithyroperoxidase antibody, body mass, protein, r-glutamyl transpeptidase, urea creatinine, mean corpuscular volume, dietary habits 1, triglyceride, immunoglobulin M, Indirect bilirubin, body mass index, operation history, carcinoembryonic antigen 1, urine creatinine, free thyroxine, hipline, PGI/PGII, plasma fibrinogen concentration, total thyroxine, urine transferri
Cervical spondylopathy	albumin, anamnesis, age, high-density lipoprotein, specific gravity, height, body mass, operation history, urine creatinine, hipline, plasma fibrinogen concentration, alanine aminotransferase, known of drug allergy, exercise habits, 5-nucleotidase, erythrocyte sedimentation rate,

	estimated glomerular filtration rate, glucose, systolic pressure, urea, urine sugar, alpha-fetoprotein, anti-cyclic peptide containing citrulline, apolipoprotein A, CD3+ Total T lymphocyte, corrected visual acuity the left eye, gastrin-17, hourly postprandial blood sugar, intra-ocular tension of the left eye, kalium, magnesium, neuron-specific enolase
Rheumatoid arthritis	albumin, anamnesis, age, high-density lipoprotein, specific gravity, height, body mass, hipline, known of drug allergy, estimated glomerular filtration rate, systolic pressure, gastrin-17, neck size, gender, history of alcohol intake, hemoglobin, protein, urea creatinine, body mass index, uric acid, monocytes, red blood cell count, red cell distribution width, albumin-globulin, mean corpuscular hemoglobin concentration, vision of the left eye, vision of the right eye, lactic dehydrogenase, lymphocyte rate, globulin, leucocyte, α hydroxybutyrate dehydrogenas
Chronic rhinitis	albumin, anamnesis, age, high-density lipoprotein, height, estimated glomerular filtration rate, systolic pressure, gender, hemoglobin, protein, urea creatinine, uric acid, albumin-globulin, mean corpuscular hemoglobin concentration, lactic dehydrogenase, 5-nucleotidase, creatinine, dietary habits 1, triglyceride, total thyroxine, free triiodothyronine, diastolic pressure, eosinophil rate, alkaline phosphatase, total cholesterol, apolipoprotein B, erythrocyte aggregation Indices, granulocyte rate, helicobacter pylori antibody-IgG, hepatitis B virus core IM antibod, quantitative detection of hepatitis B virus DNA
Nephropathy	albumin, anamnesis, age, estimated glomerular filtration rate, systolic pressure, hemoglobin, protein, urea creatinine, uric acid, albumin-globulin, lactic dehydrogenase, creatinine, eosinophil rate, known of drug allergy, monocytes, red blood cell count, red cell distribution width, lymphocyte rate, operation history, erythrocyte sedimentation rate, urea, Indirect bilirubin, waistline, monocytes %, leukocyte count, total Protein, pepsinogen I, cystatin c, calcium, adrenocorticotropic hormone, ALDH2-Glu504Lys, creatine kinase, pepsinogen II
Diabetes	albumin, anamnesis, age, estimated glomerular filtration rate, systolic pressure, urea creatinine, red cell distribution width, lymphocyte rate, operation history, urea, waistline, monocytes %, leukocyte count, high-density lipoprotein, gender, triglyceride, free triiodothyronine, diastolic pressure, body mass, neck size, body mass index, exercise habits, glucose, urine sugar, AST/ALT, smoking history, platelet count, waist-hip ratio, PH, cytokeratin-19-fragment CYFRA21-1, ketone body, osmotic pressure
Gout	anamnesis, age, estimated glomerular filtration rate, systolic pressure, urea creatinine, lymphocyte rate, waistline, monocytes %, leukocyte count, high-density lipoprotein, gender, triglyceride, diastolic pressure, body mass, neck size, body mass index, exercise habits, glucose, AST/ALT, smoking history, waist-hip ratio, PH, hemoglobin, uric acid, creatinine, red blood cell count, cystatin c, height, hipline, history of alcohol intake, alanine aminotransferase, r-glutamyl transpeptidase, aspartate transaminase
Parkinson's syndrome	anamnesis, age, estimated glomerular filtration rate, systolic pressure, lymphocyte rate, waistline, monocytes %, leukocyte count, gender, glucose, AST/ALT, waist-hip ratio, hemoglobin, creatinine, red blood cell count, history of alcohol intake, albumin, red cell distribution

	width, urea, platelet count, monocytes, total Protein, calcium, mean corpuscular hemoglobin concentration, total cholesterol, granulocyte rate, urine creatinine, urine transferrin, low-density lipoprotein, anti-Sc70, anti-U1RNP antibody, CD3+CD4+CD8+
Stomach trouble	anamnesis, age, estimated glomerular filtration rate, monocytes %, leukocyte count, waist-hip ratio, red blood cell count, red cell distribution width, platelet count, total cholesterol, urine creatinine, low-density lipoprotein, high-density lipoprotein, body mass, body mass index, exercise habits, uric acid, height, hipline, operation history, protein, known of drug allergy, specific gravity, anti Sm antibody, anti-cenpb, anti-cyclin antibody, anti-dsDNA antibody, anti-histone antibody, antimitochondrial antibody M2, anti-nucleosome antibody Systemic, anti-ribosomal p protein antibody, nitrous acid, rheumatoid factor
Chronic pharyngitis	anamnesis, red blood cell count, body mass, exercise habits, height, anti Sm antibody, anti-dsDNA antibody, anti-nucleosome antibody Systemic, anti-ribosomal p protein antibody, waistline, gender, hemoglobin, creatinine, history of alcohol intake, albumin, mean corpuscular hemoglobin concentration, urine transferrin, urea creatinine, neck size, albumin-globulin, dietary habits 1, globulin, leucocyte, whole blood high shear reduced viscosity index, bilirubin, CD3-CD19+(B cell), percentage activity of prothrombin in plasma, shear rate of whole blood viscosity_mPas (100), shear rate of whole blood viscosity_mPas (50), shear rate of whole blood viscosity_mPas_1 (200), the Index of Rigidity of Erythrocyte, total bile acid, whole blood high shear reduced viscosity
Lumbar disc protrusion	anamnesis, body mass, exercise habits, waistline, gender, creatinine, albumin, neck size, age, estimated glomerular filtration rate, waist-hip ratio, red cell distribution width, platelet count, total cholesterol, urine creatinine, low-density lipoprotein, body mass index, hipline, operation history, known of drug allergy, glucose, urea, total Protein, smoking history, eosinophil rate, mean corpuscular volume, carcinoembryonic antigen 1, free thyroxine, anion gap, basophilic granulocyte rate, homocysteine, ratio of urinary microalbumin to creatinin
Hepatitis B	anamnesis, body mass, waistline, gender, creatinine, neck size, age, estimated glomerular filtration rate, waist-hip ratio, platelet count, total cholesterol, body mass index, hipline, smoking history, eosinophil rate, basophilic granulocyte rate, ratio of urinary microalbumin to creatinin, height, hemoglobin, leukocyte count, AST/ALT, monocytes, calcium, granulocyte rate, cystatin c, alanine aminotransferase, aspartate transaminase, vision of the right eye, kalium, adenosine deaminase, direct bilirubin, microalbuminuria, prealbumin
Hypertension+other diseases	anamnesis, body mass, waistline, creatinine, neck size, age, estimated glomerular filtration rate, waist-hip ratio, body mass index, hipline, eosinophil rate, height, cystatin c, aspartate transaminase, exercise habits, albumin, red cell distribution width, operation history, known of drug allergy, glucose, urea, mean corpuscular volume, red blood cell count, albumin-globulin, globulin, monocytes %, uric acid, specific gravity, systolic pressure, triglyceride, diastolic pressure, lactic dehydrogenase
Coronary heart disease+other diseases	anamnesis, body mass, age, estimated glomerular filtration rate, waist-hip ratio, hipline, cystatin c, albumin, red cell distribution width,

	operation history, urea, red blood cell count, specific gravity, systolic pressure, platelet count, total cholesterol, hemoglobin, AST/ALT, monocytes, calcium, alanine aminotransferase, vision of the right eye, urine creatinine, low-density lipoprotein, total Protein, carcinoembryonic antigen 1, history of alcohol intake, protein, apolipoprotein B, vision of the left eye, apolipoprotein A, apolipoprotein a1/b
Diabetes+other diseases	anamnesis, age, estimated glomerular filtration rate, cystatin c, albumin, red cell distribution width, operation history, urea, systolic pressure, platelet count, urine creatinine, carcinoembryonic antigen 1, vision of the left eye, waistline, neck size, body mass index, known of drug allergy, glucose, mean corpuscular volume, gender, smoking history, dietary habits 1, high-density lipoprotein, lymphocyte rate, PH, urine sugar, cytokeratin-19-fragment CYFRA21-1, mean corpuscular hemoglobin, complexed prostate special antigen, follicle stimulating hormone, luteinizing hormone, pituitary prolactin
Bronchial disease	anamnesis, age, estimated glomerular filtration rate, albumin, red cell distribution width, operation history, urea, systolic pressure, urine creatinine, waistline, neck size, known of drug allergy, mean corpuscular volume, gender, lymphocyte rate, mean corpuscular hemoglobin, AST/ALT, apolipoprotein A, creatinine, eosinophil rate, height, exercise habits, albumin-globulin, globulin, monocytes %, lactic dehydrogenase, adenosine deaminase, bilirubin, ketone body, intra-ocular tension of the right eye
Other disease conditions	anamnesis, age, estimated glomerular filtration rate, albumin, red cell distribution width, operation history, urea, systolic pressure, waistline, neck size, known of drug allergy, mean corpuscular volume, exercise habits, albumin-globulin, platelet count, body mass index, glucose, urine sugar, red blood cell count, specific gravity, total cholesterol, hemoglobin, monocytes, calcium, total Protein, diastolic pressure, mean corpuscular hemoglobin concentration, Indirect bilirubin, pepsinogen I, pepsinogen II, total bilirubin, alpha-l-fucosidas
Brain diseases	anamnesis, age, estimated glomerular filtration rate, albumin, red cell distribution width, operation history, urea, systolic pressure, waistline, exercise habits, albumin-globulin, red blood cell count, hemoglobin, monocytes, calcium, total Protein, lymphocyte rate, AST/ALT, creatinine, monocytes %, lactic dehydrogenase, carcinoembryonic antigen 1, cytokeratin-19-fragment CYFRA21-1, follicle stimulating hormone, waist-hip ratio, vision of the right eye, whole blood high shear reduced viscosity index, adrenocorticotropic hormone, creatine kinase isoenzyme, epithelial cell, other cell types, progesterone
Hepatic adipose infiltration	anamnesis, albumin, systolic pressure, waistline, red blood cell count, hemoglobin, AST/ALT, creatinine, monocytes %, waist-hip ratio, neck size, mean corpuscular volume, body mass index, diastolic pressure, mean corpuscular hemoglobin concentration, alpha-l-fucosidase, gender, mean corpuscular hemoglobin, height, dietary habits 1, high-density lipoprotein, body mass, hipline, alanine aminotransferase, low-density lipoprotein, history of alcohol intake, aspartate transaminase, uric acid, triglyceride, leukocyte count, r-glutamyl transpeptidase, testosterone

Asthma	anamnesis, albumin, systolic pressure, waistline, red blood cell count, hemoglobin, waist-hip ratio, neck size, mean corpuscular hemoglobin concentration, gender, height, high-density lipoprotein, body mass, alanine aminotransferase, low-density lipoprotein, r-glutamyl transpeptidase, age, estimated glomerular filtration rate, red cell distribution width, albumin-globulin, total Protein, carcinoembryonic antigen 1, known of drug allergy, platelet count, specific gravity, total cholesterol, eosinophil rate, smoking history, basophilic granulocyte rate, PGI/PGII, CD3+CD16+CD56+NK, urinary nuclear matrix protein 22
Other Cardiac diseases	anamnesis, albumin, systolic pressure, waistline, red blood cell count, hemoglobin, waist-hip ratio, mean corpuscular hemoglobin concentration, gender, height, age, estimated glomerular filtration rate, red cell distribution width, albumin-globulin, known of drug allergy, platelet count, specific gravity, dietary habits 1, operation history, urea, monocytes, glucose, pepsinogen II, vision of the left eye, luteinizing hormone, direct bilirubin, urea creatinine, osmotic pressure, α hydroxybutyrate dehydrogenas, alpha-fetoprotein, magnesium, carbohydrate antigen, CA242
Heart disease	anamnesis, albumin, systolic pressure, waistline, red blood cell count, hemoglobin, waist-hip ratio, age, estimated glomerular filtration rate, red cell distribution width, albumin-globulin, platelet count, operation history, urea, monocytes, luteinizing hormone, carcinoembryonic antigen 1, creatinine, mean corpuscular volume, mean corpuscular hemoglobin, aspartate transaminase, lactic dehydrogenase, cytokeratin-19-fragment CYFRA21-1, progesterone, urine creatinine, anti-cenpb, antimitochondrial antibody M2, CD3+CD4+CD8+, anti-cyclic peptide containing citrulline, thyroid-stimulating hormon, prothrombin time, quantitative detection of hepatitis C virus RNA
Hepatopathy	anamnesis, albumin, waistline, red blood cell count, waist-hip ratio, age, estimated glomerular filtration rate, red cell distribution width, albumin-globulin, operation history, mean corpuscular volume, mean corpuscular hemoglobin, aspartate transaminase, anti-cenpb, direct bilirubin, basophilic granulocyte rate, urinary nuclear matrix protein 22, body mass index, exercise habits, other cell types, apolipoprotein a1/b, anti Sm antibody, anti-nucleosome antibody Systemic, anti-ribosomal p protein antibody, erythrocyte sedimentation rate, corrected visual acuity the left eye, anti-PM-Scl, corrected visual acuity the right eye, high sensitivity C-reactive protein 1
Pregnant	albumin, red blood cell count, age, estimated glomerular filtration rate, red cell distribution width, basophilic granulocyte rate, systolic pressure, hemoglobin, urea, monocytes, creatinine, gender, height, glucose, high-density lipoprotein, low-density lipoprotein, total Protein, smoking history, diastolic pressure, history of alcohol intake, uric acid, leukocyte count, lymphocyte rate, Indirect bilirubin, total bilirubin, cystatin c, protein, granulocyte rate, leucocyte, rheumatoid factor, quantitative detection of hepatitis B virus DNA , CD3+ Total T lymphocyte, anti cardiolipin antibodyIg(G-A-M)
Helathy or combined disease s	albumin, age, estimated glomerular filtration rate, red cell distribution width, systolic pressure, urea, monocytes, creatinine, gender, height,

	glucose, high-density lipoprotein, smoking history, diastolic pressure, uric acid, lymphocyte rate, cystatin c, anamnesis, waistline, albumin-globulin, operation history, body mass index, exercise habits, platelet count, known of drug allergy, neck size, body mass, monocytes %, hipline, triglyceride, urine sugar, globulin

Extended data Table 3. Predictive Validity of Models. The number of training set and valid set samples was obtained after undersampling and data random splitting. Normal condition or disease was used to classify all kinds of diseases into disease states, undersampling with samples of healthy people, and then data division. Abbreviation: receiver operating characteristic, ROC; AUC, area under the curve.

	Training set (sample size)	Validation set (sample size)	F1-score (95%CI)	Accuracy (95%CI)	Specificity (95%CI)	Recall (sensitivity)(95%CI)	ROC(AUC)(95%CI)
Cholecystolithiasis	963	413	0.69(0.66-0.71)	0.69(0.68-0.71)	0.73(0.70-0.76)	0.70(0.67-0.72)	0.77(0.75-0.79)
Hypertension	46171	17987	0.86(0.86-0.86)	0.85(0.85-0.86)	0.82(0.82-0.82)	0.85(0.85-0.86)	0.92(0.92-0.93)
Hypertension+Diabetes	8414	3065	0.92(0.92-0.92)	0.92(0.92-0.92)	0.90(0.90-0.90)	0.92(0.92-0.92)	0.97(0.97-0.98)
Hypertension+Coronary heart disease	2032	871	0.93(0.92-0.93)	0.93(0.92-0.93)	0.90(0.90-0.91)	0.93(0.92-0.93)	0.97(0.97-0.98)
Hypertensive+Diabetes+Coronary Heart Disease	909	389	0.96(0.95-0.96)	0.95(0.94-0.97)	0.95(0.94-0.95)	0.95(0.94-0.97)	0.99(0.98-0.99)
Hyperlipidemia	1687	722	0.86(0.85-0.86)	0.85(0.84-0.86)	0.82(0.81-0.83)	0.85(0.84-0.86)	0.94(0.93-0.94)
Coronary heart disease	1298	557	0.90(0.89-0.92)	0.90(0.88-0.91)	0.87(0.84-0.89)	0.90(0.88-0.91)	0.96(0.96-0.97)
Coronary heart disease+Diabetes	274	118	0.93(0.93-0.94)	0.94(0.92-0.96)	0.91(0.88-0.95)	0.94(0.92-0.95)	0.98(0.97-1.00)
Rhinallergosis	152	66	0.71(0.64-0.79)	0.69(0.61-0.79)	0.80(0.73-0.86)	0.70(0.64-0.76)	0.79(0.73-0.84)
Hypothyroidism	1627	698	0.77(0.76-0.78)	0.76(0.75-0.76)	0.73(0.71-0.74)	0.76(0.75-0.76)	0.84(0.83-0.86)
Hyperthyroidism	751	322	0.72(0.71-0.72)	0.73(0.71-0.74)	0.73(0.71-0.75)	0.73(0.71-0.74)	0.79(0.77-0.81)
Cervical spondylopathy	311	134	0.71(0.66-0.75)	0.71(0.69-0.73)	0.73(0.64-0.81)	0.71(0.69-0.73)	0.78(0.78-0.80)
Rheumatoid arthritis	387	167	0.79(0.78-0.81)	0.78(0.77-0.78)	0.76(0.71-0.81)	0.78(0.77-0.79)	0.86(0.83-0.89)
Chronic rhinitis	313	135	0.61(0.58-0.64)	0.60(0.58-0.62)	0.57(0.56-0.57)	0.61(0.58-0.63)	0.66(0.60-0.72)
Nephropathy	564	242	0.73(0.72-0.74)	0.77(0.75-0.80)	0.81(0.79-0.84)	0.76(0.75-0.78)	0.84(0.82-0.85)
Diabetes	11545	4949	0.90(0.90-0.90)	0.90(0.90-0.90)	0.90(0.89-0.90)	0.90(0.90-0.90)	0.96(0.96-0.96)
Gout	2095	898	0.88(0.88-0.88)	0.87(0.87-0.87)	0.85(0.84-0.87)	0.86(0.83-0.88)	0.94(0.94-0.94)
Parkinson's syndrome	192	83	0.91(0.90-0.91)	0.90(0.89-0.90)	0.87(0.79-0.94)	0.90(0.89-0.91)	0.97(0.95-0.98)
Stomach trouble	1269	545	0.68(0.68-0.69)	0.70(0.70-0.70)	0.71(0.70-0.73)	0.70(0.70-0.70)	0.77(0.75-0.78)
Chronic pharyngitis	765	329	0.63(0.62-0.65)	0.67(0.65-0.69)	0.66(0.65-0.66)	0.67(0.65-0.68)	0.72(0.69-0.75)

Lumbar disc protrusion	377	162	0.77(0.72-0.81)	0.77(0.73-0.80)	0.70(0.63-0.77)	0.75(0.70-0.79)	0.85(0.82-0.88)
Hepatitis B	691	297	0.73(0.70-0.77)	0.75(0.73-0.77)	0.79(0.77-0.80)	0.75(0.72-0.77)	0.83(0.81-0.85)
Hypertension+other diseases	2360	1012	0.86(0.85-0.88)	0.85(0.85-0.86)	0.82(0.81-0.83)	0.86(0.85-0.86)	0.93(0.93-0.94)
Coronary heart disease+other diseases	98	43	0.88(0.84-0.92)	0.87(0.84-0.89)	0.83(0.76-0.90)	0.86(0.83-0.88)	0.94(0.91-0.97)
Diabetes+other diseases	365	157	0.90(0.87-0.94)	0.90(0.87-0.94)	0.89(0.84-0.94)	0.90(0.86-0.94)	0.96(0.93-0.98)
Bronchial disease	562	241	0.76(0.70-0.83)	0.77(0.70-0.83)	0.80(0.76-0.84)	0.77(070-0.83)	0.83(0.79-0.88)
Other disease conditions	2720	1167	0.68(0.67-0.70)	0.69(0.67-0.71)	0.69(0.66-0.73)	0.69(0.67-0.71)	0.75(0.74-0.77)
Brain diseases	251	108	0.86(0.81-0.90)	0.86(0.82-0.91)	0.83(0.75-0.90)	0.87(0.82-0.91)	0.93(0.91-0.95)
Hepatic adipose infiltration	803	115	0.82(0.78-0.87)	0.81(0.76-0.86)	0.75(0.67-0.82)	0.82(0.77-0.87)	0.92(0.89-0.94)
Asthma	1640	803	0.75(0.74-0.76)	0.74(0.73-0.76)	0.77(0.69-0.84)	0.75(0.74-0.76)	0.88(0.84-0.92)
Other Cardiac diseases	336	145	0.79(0.78-0.81)	0.78(0.76-0.80)	0.80(0.75-0.86)	0.78(0.76-0.80)	0.88(0.84-0.92)
Heart disease	224	96	0.89(0.87-0.90)	0.89(0.85-0.92)	0.91(0.87-0.94)	0.89(0.86-0.92)	0.94(0.90-0.99)
Hepatopathy	176	76	0.71(0.65-0.76)	0.72(0.66-0.78)	0.78(0.68-0.87)	0.73(0.68-0.78)	0.80(0.74-0.85)
Pregnant	54	24	0.83(0.76-0.90)	0.82(0.76-0.88)	0.85(0.79-0.92)	0.82(0.77-0.86)	0.91(0.90-0.93)
Normal or non-normal condition	91028	39012	0.83(0.83-0.83)	0.82(0.82-0.82)	0.81(0.81-0.81)	0.84(0.84-0.84)	0.9(0.90-0.90)

Extended data Figure 1. **PEI networks in hypertension (a) and diabetes (b)**. In weighted graphs, green edges indicate positive weights, and red edges indicate negative weights. The color saturation and the width of the edges correspond to the absolute weight and scale relative to the strongest weight in the graph. At a minimum, the edge with absolute weight at this value is omitted. The circular layout is convenient to see how well the data conform to a model, but in order to show how the data clusters, another layout is more appropriate. A force-oriented layout was created by specifying layout = "spring". In principle, what this function does is that each node (connected and unconnected) repulses each other, and connected nodes also attract each other. The full view of these figures is provided in Supplementary Figures.

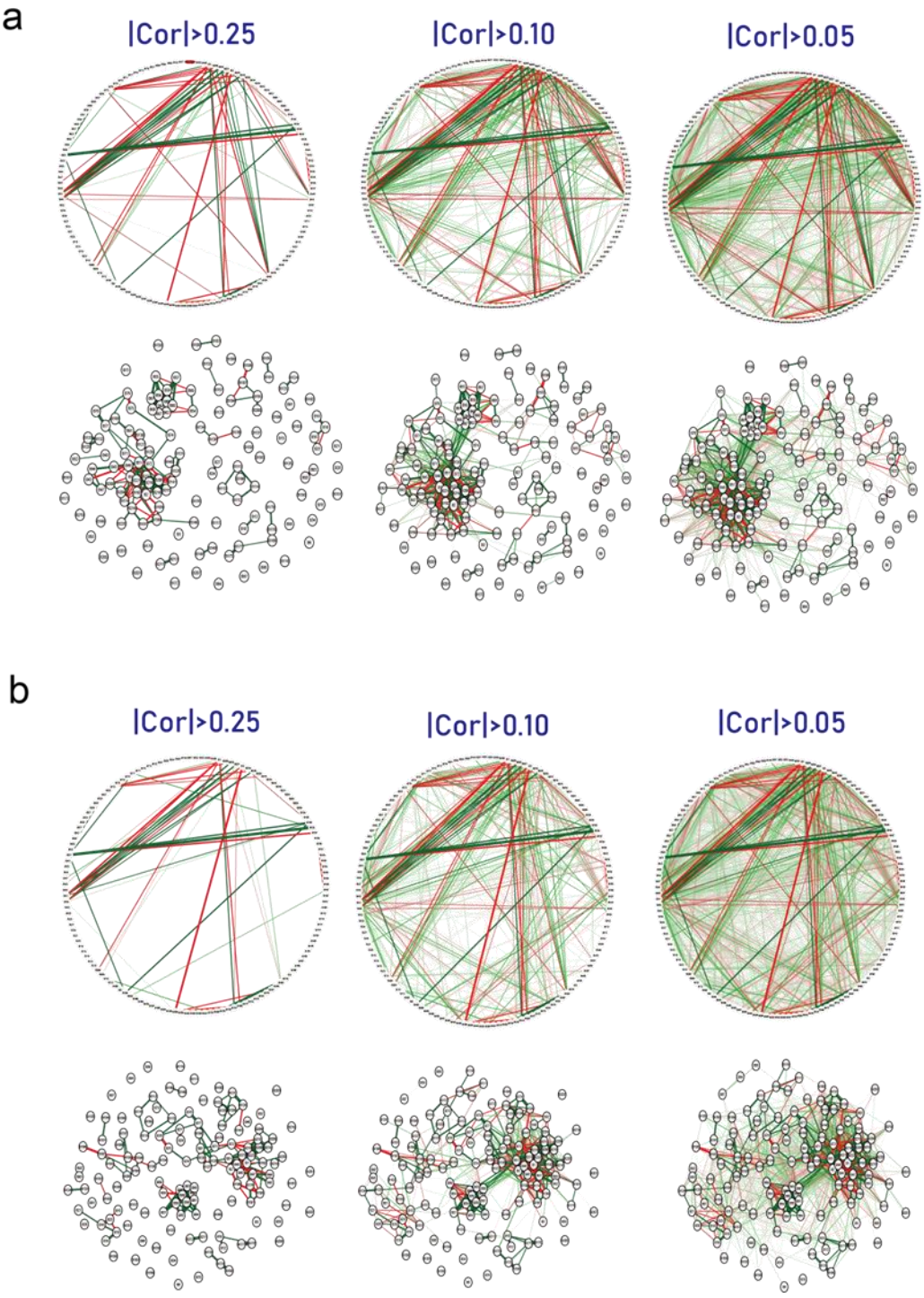

Extended data Figure 2. Odds ratios for HDL-C concentration in plasma from those with a normal physical status and those with diabetes. Both male and female subjects were included in this study.

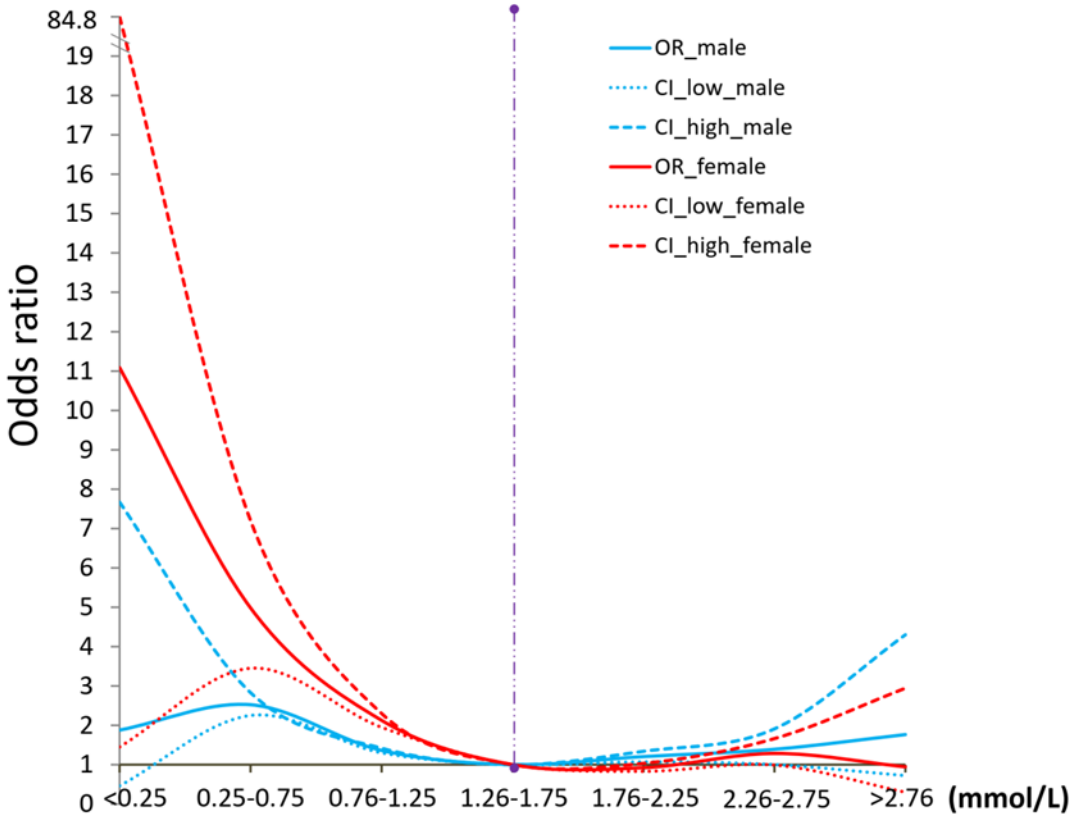

Supplementary Tables

Supplementary codes